Fluctuation-induced vortex pattern and its disordering in the fully frustrated *XY* model on a dice lattice

S. E. Korshunov
L. D. Landau Institute for Theoretical Physics, Kosygina 2, Moscow 119334, Russia
(Received 27 October 2004; published 3 May 2005)

A highly degenerate family of states, in which the adjacent plaquettes with the same sign of vorticity form clusters of three [proposed in Phys. Rev. B **63**, 134503 (2001)], is proven to really minimize the Hamiltonian of the fully frustrated *XY* model on a dice lattice. The harmonic fluctuations are demonstrated to be of no consequence for the removal of the accidental degeneracy of these states, so a particular vortex pattern can be stabilized only by the anharmonic fluctuations. The structure of this pattern is found and the temperature of its disordering due to the proliferation of domain walls is estimated. The extreme smallness of the fluctuation-induced free energy of domain walls leads to the anomalous prominence of the finite-size effects, which prevents the observation of vortex-pattern ordering in numerical simulations. In such circumstances the loss of phase coherence may be related to the dissociation of pairs of fractional vortices with the topological charges $\pm 1/8$. In a physical situation the magnetic interactions of currents in a Josephson junction array will be a more important source for the stabilization of a particular vortex pattern then the anharmonic fluctuations.

DOI: 10.1103/PhysRevB.71.174501 PACS number(s): 74.81.Fa, 64.60.Cn, 05.20.−y

I. INTRODUCTION

The uniformly frustrated *XY* model has been introduced by Teitel and Jayaprakash[1] for the description of a regular array of superconducting islands connected with each other by Josephson junctions (a Josephson junction array[2]) in the presence of a uniform magnetic field. During the last two decades the main attention has been concentrated on the investigation[3–16] of so-called fully frustrated models (on various lattices), which in terms of array correspond to having a half-integer number of the superconducting flux quanta per plaquette.[3] The models belonging to this class can be also used for the description of a planar magnet in which the neighboring spins can have either ferromagnetic or antiferromagnetic interaction, the number of the antiferromagnetic bonds in each plaquette being odd.[17]

The ground states of the uniformly frustrated *XY* models are characterized by the combination of the continuous and discrete degeneracies.[1] The former is related to the invariance of energy with respect to the global phase rotation, whereas the latter can be discussed in terms of the formation of a particular vortex pattern. In the fully frustrated models the numbers of plaquettes which contain positive and negative vortices should be equal to each other.

Since vortices of the same signs repel each other, the energy is minimized when the vorticities of neighboring plaquettes are of the opposite signs. On a square lattice this requirement can be simultaneously satisfied for all pairs of neighboring plaquettes, which allows one to conclude that the ground state has the checkerboard structure and a twofold discrete degeneracy.[17] With increase of temperature two different phase transitions can be expected to take place,[3] one of which is related to the loss of phase coherence and the other can be associated with vortex-pattern disordering. The analysis of the mutual influence between the two types of topological excitations shows that in the case of a square lattice the former has to take place at lower temperature than the latter.[14]

A triangular lattice also allows for the construction of a doubly degenerate pattern in which the vorticities are of the opposite signs for all pairs of neighboring plaquettes.[4,5] It turns out to be possible to demonstrate that the thermodynamic properties of the fully frustrated *XY* model on a triangular lattice (including the sequence of phase transitions) are completely analogous to those of the model on a square lattice.[14]

On a honeycomb lattice the situation is more complex because the family of ground states of the fully frustrated *XY* model is characterized by an infinite accidental degeneracy,[6] which can be described in terms of the formation of parallel zero-energy domain walls.[9,10,18] In such a case the structure of the vortex pattern at low, but finite temperatures cannot be determined without taking into account the contribution to free energy from the small amplitude fluctuations in the vicinities of different ground states. This mechanism of the removal of an accidental degeneracy[19,20] is often referred to as "order-from disorder." In systems with a continuous degeneracy it is usually sufficient to compare the contributions from harmonic fluctuations.[20–22]

Recently it has been discovered that in the fully frustrated *XY* model on a honeycomb lattice the order-from-disorder mechanism does not work at the harmonic level.[16] The difference between the free energies of fluctuations appears only when one takes into account the anharmonicities, and, as a consequence, is proportional not to the first, but to the second power of temperature. This feature leads to the unusual prominence of the finite-size effects.[16]

The present work is devoted to the investigation of the fully frustrated *XY* model on a dice lattice[23] (see Fig. 1). Like square, triangular, and honeycomb lattices, the dice lattice consists of identical plaquettes (which in this case are rhombic) and equivalent bonds. Since the invariant description of a Josephson junction array can be achieved only in terms of variables which are defined on lattice bonds [the gauge-invariant phase differences, see Eq. (4)], and not on sites, the

dice lattice can be considered as one of the four basic lattices for the investigation of the uniformly frustrated *XY* models. On more complex lattices (containing nonequivalent plaquettes) the correspondence between an array and a frustrated *XY* model is likely to be broken as a consequence of the phenomenon of the "hidden incommensurability," related to the redistribution of magnetic field between the plaquettes by screening currents in asymmetric superconducting islands.[24,25]

Recently a hypothesis has been but forward[13] that in the ground states of the fully frustrated *XY* model on a dice lattice the vortices of the same sign form three-vortex clusters (triads), and a highly degenerate family of states has been proposed, which satisfies this criterion and can be described in terms of the formation of a network of intersecting zero-energy domain walls. In Sec. II we present a rigorous proof that these states indeed correspond to the absolute minimum of energy.

Section III is devoted to the analysis of harmonic fluctuations. We reveal the existence of a hidden gauge symmetry, which allows one to conclude that for a particular choice of boundary conditions the set of the eigenvalues of the harmonic Hamiltonian is exactly the same for all ground states. As a consequence, the free energy of the harmonic fluctuations cannot be the source for the selection of a particular vortex pattern. This conclusion is valid also for quantum generalizations of the model. All these properties resemble very much the analogous properties of the fully frustrated *XY* model on a honeycomb lattice.[16]

In Sec. IV the lowest order contribution to the free energy of anharmonic fluctuations is considered. In particular, the gauge symmetry mentioned above is applied to demonstrate that the contribution related to the fourth-order terms in the Hamiltonian is the same for all ground states and, therefore, is of no consequence for the selection of a particular vortex pattern. The continuous approximation is used to show that the fluctuation-induced interaction of zero-energy domain walls is extremely weak and decays inversely proportionally to the fifth power of the distance between them. The comparison of the numerically calculated free energies of anharmonic fluctuations in different periodic ground states allows us to establish the vortex pattern which can be expected to be stabilized at low temperatures and to find the fluctuation-induced free energy of zero-energy domain walls.

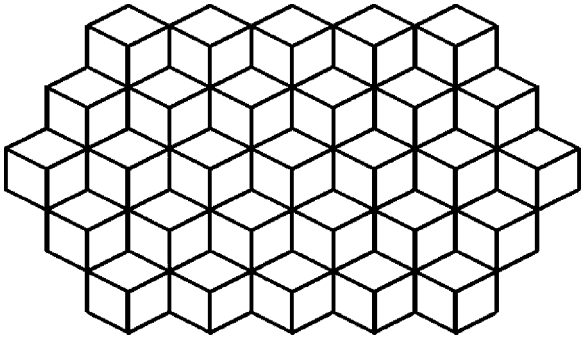

FIG. 1. Dice lattice is the simplest periodic lattice which can be constructed from identical rhombic plaquettes with three different orientations.

In Sec. V we analyze how the vortex pattern selected by anharmonic fluctuations becomes disordered when one takes into account the fluctuations of another type, namely, the formation of domain walls, and propose an estimate for the temperature of the phase transition which can be associated with the proliferation of such defects. In this section we also discuss the finite-size effects which interfere with the observation of vortex-pattern ordering in finite samples and show that in the considered system they are extremely prominent (exactly for the same reasons as in the case of a honeycomb lattice).

In Sec. VI the interplay between the vortex-pattern disordering and the loss of phase coherence is considered, whereas Sec. VII is devoted to a discussion of another mechanism of the removal of an accidental degeneracy related to magnetic interactions of currents in the array.[25,26] In the concluding Sec. VIII our results are summarized and compared with the results of numerical simulations of Cataudella and Fazio.[15]

The interest in magnetically frustrated systems with dice lattice geometry has appeared after Vidal *et al.*[27] discovered that at full frustration the ground state of a single electron, which can jump between the nearest sites of a dice lattice, is infinitely degenerate and that the corresponding wave function can be chosen as an arbitrary linear combination of an infinite number of extremely localized wave functions, each of which covers only a finite (and small) number of sites. Since it is known that the structure of the superconducting state in a wire network is determined (in the mean-field approximation) by the structure of the ground-state wave function of the single-electron problem with the same geometry,[28] a suggestion has been put forward that at full frustrateion the superconducting state in a dice network may have a disordered (glassy-like) structure.[27,29] However, recently it has been shown[26] that the inclusion into analysis of the forth-order term of the Ginzburg-Landau functional strongly decreases the ambiguity in the determination of the structure of the superconducting state in a fully frustrated wire network with the dice lattice geometry. The set of states minimizing the free energy of such a network turns out to be in one-to-one correspondence with the set of the ground states of the fully frustrated *XY* model discussed in this paper. In recent years magnetically frustrated wire networks and Josephson junction arrays with the dice lattice geometry have both been the subject of active experimental investigations.[29–31]

II. THE MODEL AND THE GROUND STATES

A. The definition of the model

A uniformly frustrated *XY* model[1] can be defined by the Hamiltonian[32]

$$H = -J\sum_{(jk)} \cos(\varphi_k - \varphi_j - A_{jk}), \tag{1}$$

where the summation is performed over all bonds (jk) of a regular two-dimensional lattice. In terms of a Josephson junction array J is the Josephson coupling constant of a single junction, fluctuating variables φ_j are the phases of the

order parameter on superconducting grains j forming the array, whereas quenched variables,

$$A_{jk} = \frac{2\pi}{\Phi_0}\int_{\mathbf{r}_j}^{\mathbf{r}_k} d\mathbf{r}\mathbf{A}(\mathbf{r}), \tag{2}$$

are defined by the integral of the vector potential $\mathbf{A}(\mathbf{r})$ of the external magnetic field along the bond (jk), Φ_0 being the superconducting flux quantum. The form of Eq. (1) assumes that the currents in the array are sufficiently small, so their proper magnetic fields can be neglected.

When the magnitude of the field corresponds to a half-integer number of flux quanta per plaquette, the directed sum of $A_{jk} \equiv -A_{kj}$ along the perimeter of a plaquette in the positive direction (which below is designated as $\Sigma_\square$) has to satisfy the constraint

$$\sum_\square A_{jk} = \pi (\mathrm{mod}\ 2\pi) \tag{3}$$

on each plaquette of the lattice. In such a case the model is called fully frustrated.[3] In a more general case of a uniformly frustrated XY model, the right-hand side of Eq. (3) should be replaced by $2\pi f (\mathrm{mod}\ 2\pi)$, where the frustration parameter f describes the magnitude of the external magnetic field in terms of the number of flux quanta per plaquette. It is sufficient to consider the interval $f \in [0, \frac{1}{2}]$, because all other values of f can be reduced to this interval by a simple replacement of variables.[1] The term "fully frustrated" is used for the case of $f=1/2$, the maximal irreducible value of f.

Since both variables φ_j and variables A_{jk} depend on a choice of a gauge, it is often more convenient to describe different states of the system in terms of the gauge-invariant phase differences,

$$\theta_{jk} = \varphi_k - \varphi_j - A_{jk} \equiv -\theta_{kj}, \tag{4}$$

defined on lattice bonds. Below we will always assume θ_{jk} to be reduced to the interval $(-\pi, \pi)$. It follows from the definition of these variables that in the fully frustrated model they have to satisfy the constraints,

$$\sum_\square \theta_{jk} = \pi (\mathrm{mod}\ 2\pi), \tag{5}$$

completely analogous to Eq. (3). One usually says that a given plaquette contains a positive (or negative) half-vortex when the left-hand side of Eq. (5) is equal to $+\pi$ (or $-\pi$). Different minima of the Hamiltonian (1) (including the ground states) can be then identified in terms of a corresponding vortex configuration.

The variation of Eq. (1) with respect to φ_j results in the current conservation equation for the site j, the value of the current in the junction (jk) being given by

$$I_{jk} = I_0 \sin \theta_{jk}, \tag{6}$$

where $I_0 = (2e/\hbar)J$ is the critical current of a single junction.

B. Minimization of energy

The dice lattice (Fig. 1) is formed by two types of sites, with the coordination numbers three and six, connected with each other in such a way that each bond connects two sites with different coordination numbers. Below we will always use index k to denote the threefold coordinated sites of a dice lattice and index j to denote the sixfold coordinated sites. For example, the bond (jk) connects the sixfold coordinated site j with the threefold coordinated site k.

The minimization of the Hamiltonian (1) with respect to all variables φ_k for the given values of the variables φ_j can be performed exactly. To describe the result of this procedure it is convenient to introduce also the gauge-invariant phase differences $\chi_{jj'} \equiv -\chi_{j'j}$ defined on the bonds of the triangular lattice $\mathcal{T}$ formed by the sixfold coordinated sites j. A natural way to do it consists of requiring that for each triangle formed by the sites j, j', and k (where j and j' are the nearest neighbors of k) the sum of the three gauge-invariant phase differences taken along its perimeter in the positive direction should be equal to $\pm\pi/2$ modulo 2π, where the sign should be the same for all triangles. In what follows we assume this sign to be negative,

$$\chi_{jj'} + \theta_{j'k} + \theta_{kj} = -\pi/2 (\mathrm{mod}\ 2\pi). \tag{7}$$

Since $\chi_{jj'} = -\chi_{j'j}$, the constraint (5) then automatically follows from Eq. (7). On the other hand, on each triangular plaquette of $\mathcal{T}$ the directed sum of the variables $\chi_{jj'}$ has to satisfy the constraint

$$\sum_\square \chi_{jj'} = \pi/2 (\mathrm{mod}\ 2\pi), \tag{8}$$

which can be obtained by summation of Eq. (7) for three neighboring triangles with the common cite k.

The minimization of

$$E_k = -J\sum_{a=1}^{3} \cos \theta_{j_a k}$$

(where j_a with $a=1,2,3$ are the three nearest neighbors of k on a dice lattice numbered in the positive direction) with respect to φ_k for the given values of $\chi_{j_1 j_2}$, $\chi_{j_2 j_3}$, and $\chi_{j_3 j_1}$ satisfying the constraint (8) gives

$$E_k = -J\sqrt{3 - 2Y_k}$$

where

$$Y_k = \sin \chi_{j_1 j_2} + \sin \chi_{j_2 j_3} + \sin \chi_{j_3 j_1} \leqslant 3/2.$$

Since $E(Y) = -J\sqrt{3-2Y}$ is a concave function of Y and the sum of the variables Y_k over the whole lattice with the periodic boundary conditions should be equal to zero, the absolute minimum of

$$H = \sum_k E(Y_k)$$

on such a lattice is achieved when $Y_k = 0$ for all k. In the next section we demonstrate that this requirement can be simultaneously satisfied on all plaquettes. Accordingly, the value of energy in the absolute minimum is given by $E = -2\sqrt{3}JN$, where N is the total number of the sixfold coordinated sites.

C. Construction of ground states

In the case of an isolated triangle the system of two equations

$$\chi_1 + \chi_2 + \chi_3 = \pi/2,$$

$$\sin\chi_1 + \sin\chi_2 + \sin\chi_3 = 0,$$

for three variables χ_1, χ_2, and χ_3 has an infinite number of solutions. However, the requirement to match the solutions on all triangular plaquettes of $\mathcal{T}$ leads to the removal of this continuous degeneracy.

Since the form of the constraint (8) corresponds to having one-quater of flux quantum per plaquette, the minimal elementary cell whose periodic repetition allows one to construct a periodic solution consists of four triangles. Such a solution can be described by six variables χ_i. Figure 2(a) shows how they can be defined for a particular choice of the shape of an elementary cell. These six variables have to satisfy three flux quantization constraints of the form given by Eq. (8):

$$\chi_1 + \chi_2 + \chi_3 = \pi/2, \tag{9a}$$

$$\chi_4 + \chi_5 + \chi_6 = \pi/2, \tag{9b}$$

$$-\chi_3 - \chi_4 - \chi_5 = \pi/2, \tag{9c}$$

and three equations of the form $Y_k=0$:

$$\sin\chi_1 + \sin\chi_2 + \sin\chi_3 = 0, \tag{10a}$$

$$\sin\chi_4 + \sin\chi_5 + \sin\chi_6 = 0, \tag{10b}$$

$$-\sin\chi_3 - \sin\chi_4 - \sin\chi_5 = 0, \tag{10c}$$

which, according to the results of Sec. II B, is required for the minimization of energy. The fourth constraint,

$$-\chi_1 - \chi_2 - \chi_6 = -3\pi/2,$$

and the fourth equation of the form $Y_k=0$,

$$-\sin\chi_1 - \sin\chi_2 - \sin\chi_6 = 0,$$

are then satisfied automatically, as follows from the summation of Eqs. (9) and Eqs. (10), respectively.

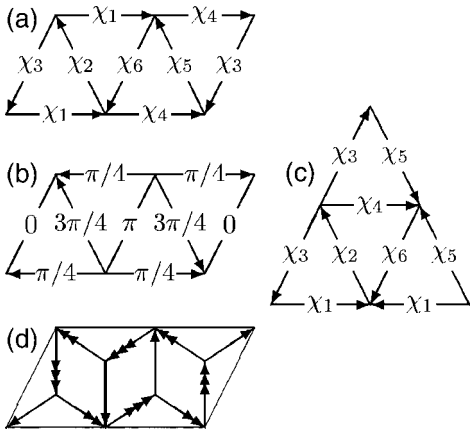

FIG. 2. Construction of a periodic ground state: (a) a possible structure of an elementary cell; (b) one of the solutions of Eqs. (9) and (10); (c) an alternative elementary cell; and (d) the same elementary cell as in (b), but in terms of θ_{jk}.

We have found that the numerical solution of the system of six equations [Eqs. (9) and (10)] by an iterative method always converges to the solution shown in Fig. 2(b) or to another analogous solution in which variables χ are equal to 0, $-\pi/4$, and $3\pi/4$ on one-half of the triangular plaquettes and to π, $\pi/4$, and $3\pi/4$ on the other half. Note that each variable χ belongs to two neigboring plaquettes, but manifests itself on them with the opposite signs. The same results are also obtained when one assumes that the elementary cell has a different shape, shown in Fig. 2(c).

Quite remarkably, an attempt to construct a solution with a larger elementary cell leads to an overdefined system of equations. For example, an elementary cell consisting of eight triangles requires one to introduce 12 variables χ_i which have to satisfy seven independent constraints of the form (8) and seven independent equations of the form $Y_k=0$. Apparently, one cannot expect a system of 14 equations for 12 variables to have a nontrivial solution which cannot be constructed from the solutions obtained for a four-triangle elementary cell. Thus the reduction of the problem to a triangular lattice has allowed us to make a conclusion on the size of the elementary cell which would be hardly possible in the framework of analysis in terms of the original variables θ_{jk} defined on the bonds of a dice lattice.

In Fig. 2(d) the structure of the elementary cell of Fig. 2(b) is shown in terms of the variables θ_{jk}. Here single, double, and triple arrows correspond, respectively, to three different values of θ_{jk},

$$\theta_{1,3} = \arccos\left(\frac{1}{\sqrt{3}} \pm \frac{1}{\sqrt{6}}\right), \quad \theta_2 = \arccos\left(\frac{1}{\sqrt{3}}\right),$$

satisfying the constraints

$$\theta_2 - \theta_1 = \pi/4, \quad \theta_1 + \theta_3 = \pi/2, \quad \theta_2 + \theta_3 = 3\pi/4,$$

which lead to the fulfilment of Eq. (5) on all rhombic plaquettes, and the current conservation equation,

$$\sin\theta_1 + \sin\theta_2 = \sin\theta_3,$$

the form of which follows from Eq. (6).

The most compact way of illustrating a structure of a given state (a local or global minimum of the Hamiltonian) consists of showing which plaquettes are occupied by positive and which plaquettes by negative half-vortices. In Fig. 3(a) this approach is used to demonstrate the structure of the ground state which is obtained by the periodic repetition of the elementary cell shown in Fig. 2(d). Notice that positive and negative half-vortices are grouped into clusters of three (triads). The rules which allow one to restore the values of θ_{jk} for each bond from the structure of the vortex pattern (in a ground state) can be found in Ref. 13.

Since positive and negative half-vortices can be considered as occuping the cites of the dual lattice (which in the present case is a *kagome* lattice), the structure of a given state of the fully frustrated *XY* model on a dice lattice can be compared with the structures of different states of the anti-

ferromagnetic Ising model on a *kagome* lattice. In particular, according to Wolf and Schotte,[33] in the framework of the Ising model the state with the structure shown in Fig. 3(a) is selected when $\mathcal{J}_1 \gg \mathcal{J}_2 \gg \mathcal{J}_4 > 0$ and all other couplings are equal to zero. Here $\mathcal{J}_i$ is the coupling constant for ith neighbors on a *kagome* lattice, and we have used the notation of Ref. 26 for the classification of dice lattice plaquettes as neighbors of each other.

The ground state whose structure is shown in Figs. 2(d) and 3(a) allows for the creation of infinite domain walls which brake the periodicity of this state but does not cost any energy.[13] These zero-energy domain walls can be of the two types.

Figure 3(b) shows an example of a zero-energy domain wall of the type I. Note that the orientations of triads formed by negative half-vortices (white plaquettes) are different above and below the wall. The configuration of arrows (defining the values of the variables θ_{jk}) after crossing such a wall can be obtained from the old configuration (in the absence of the wall) by its reflection with respect to a line which is perpendicular to the wall and subsequent inversion of all arrows. There can exist an arbitrary number of such domain walls in parallel to each other. By creating them at every possible position one obtains another periodic ground state shown in Fig. 3(c).

Figure 3(d) shows an example of zero-energy domain wall of the type II. After crossing such a wall the variables θ are changed (in comparison with what they would be in the absence of the wall) according to an even more simple rule, which can be codified as

$$\theta_1 \to \theta_3, \quad \theta_3 \to \theta_1, \quad \theta_2 \to -\theta_2. \tag{11}$$

Note that both black and white triads have different orientations on two sides of the wall, whereas at the wall the shape of white triads is modified.

Again, there can exist an arbitrary number of the type II domain walls parallel to each other. By inserting them at every possible position one obtains one more periodic ground state shown in Fig. 3(e), in which all triads have the modified shape. Alternatively, one can start the whole construction from the periodic state of Fig. 3(e) and obtain the state of Fig. 3(a) by introducing a dense sequence of domain walls on crossing which the same rule, Eq. (11), is applicable.

The zero-energy domain walls of different types can cross each other without increasing energy. However, it follows from the rule for the transformation of the state induced by the type I domain wall (described above) that a type II domain wall should change its orientation by $\pi/3$ each time it crosses a type I domain wall [see Fig. 3(f)]. A dense network of zero-energy domain walls of both types constructed on the background of state (a) leads to the periodic ground state shown in Fig. 3(g). The structures of the periodic states (a), (c), (e), and (g) in terms of the variables θ_{jk} are shown in Fig. 3 of Ref. 26.

Note that the formation of zero-energy domain walls is related to the changes of the orientation of vortex triads (and, in the case of type II domain walls, also of their shapes), but does not lead to the appearance of vortex clusters of other sizes.

III. HARMONIC APPROXIMATION

A. Two families of eigenmodes

The Hamiltonian describing the harmonic fluctuations in the vicinity of one of the ground states described in Sec. II C can be written as

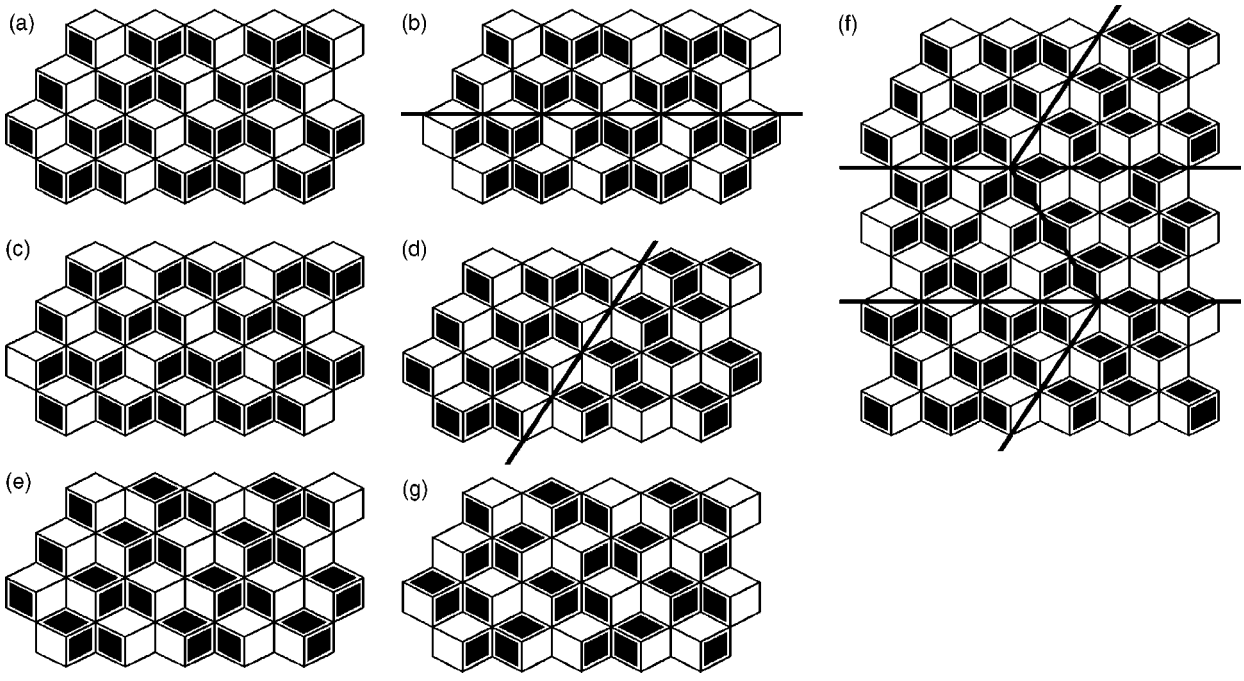

FIG. 3. The structure of some ground states. The plaquettes with positive vorticities are marked in black.

$$H^{(2)} = \frac{1}{2}\sum_{(jk)} J_{jk}(u_j - v_k)^2, \tag{12}$$

where u_j are deviations of the variables φ_j from their equilibrium values on sixfold coordinated sites, v_k are analogous deviations on threefold coordinated sites and the coupling constants $J_{jk} \equiv J \cos\theta_{jk}$ acquire one of the three possible values

$$J_{1,3} = \left(\frac{1}{\sqrt{3}} \pm \frac{1}{\sqrt{6}}\right)J, \quad J_2 = \frac{J}{\sqrt{3}}, \tag{13}$$

in accordance with the value of θ_{jk} on the bond (jk).

If phase dynamics in a Josephson junction array can be assumed to be nondissipative and the capacitance matrix of the array has only diagonal elements, the linearized equations of motion for the variables u_j and v_k following from Eq. (12) can be written as

$$(2J_S - M_6\omega^2)u_j = \sum_{k=k(j)} J_{jk}v_k, \tag{14a}$$

$$(J_S - M_3\omega^2)v_k = \sum_{j=j(k)} J_{jk}u_j, \tag{14b}$$

where $J_S = J_1 + J_2 + J_3$, $M_i = (\hbar/2e)^2 C_i$ (where $i = 3, 6$), and $j(k)$ denotes the nearest neighbors of k. In Eqs. (14) we have performed the Fourrier transformation to the frequency representation and have assumed that the self-capacitances of the superconducting islands, C_3 and C_6, are different for the two types of islands.

Note that in all ground states discussed in Sec. II C the coupling constants J_{jk} always have the same three values (J_1, J_2, and J_3) on the three bonds $(j_a k)$ connected to any site k, as a consequence of which the coefficient standing in the left-hand side of Eq. (14b) does not depend on k. This allows one to conclude that all eigenmodes with $u_j \equiv 0$ should have the same eigenfrequency $\omega_0 = (J_S/M_3)^{1/2}$. In the thermodynamic limit the degeneracy of this eigenfrequency is equal to one-third of the total number of modes.

The spectrum of the brunch with $u_j \neq 0$ can be found from the equation which is obtained after substitution of Eq. (14b) into Eq. (14a) and can be written as

$$\Lambda(\omega)u_j = \sum_{j'=j'(j)} K_{jj'}(u_j - u_{j'}), \tag{15}$$

where

$$\Lambda(\omega) = (2M_3 + M_6)\omega^2 - \frac{M_3 M_6}{J_S}\omega^4, \tag{16}$$

$j'(j)$ are the six nearest neighbors of j on $\mathcal{T}$ and

$$K_{jj'} = (J_{jk'}J_{j'k'} + J_{jk''}J_{j'k''})/J_S, \tag{17}$$

k' and k'' being the two threefold coordinated sites belonging to the same rhombic plaquette as j and j'.

The right-hand side of Eq. (15) has exactly the same form as the equation describing harmonic fluctuations on a triangular lattice with the nearest-neighbor interaction characterized by the coupling constants $K_{jj'}$ defined by Eq. (17). Quite remarkably, in all the ground states described above these coupling constants acquire only two values,

$$K_1 = \frac{2J_1J_3}{J_S} = \frac{J}{3\sqrt{3}}, \tag{18a}$$

$$K_2 = \frac{(J_1 + J_3)J_2}{J_S} = \frac{2J}{3\sqrt{3}}, \tag{18b}$$

which differ from each other by a factor of 2. When a half-vortex in the plaquette $\langle jk'j'k''\rangle$ is the central vortex of a triad to which it belongs, $K_{jj'} = K_1$, whereas otherwise $K_{jj'} = K_2$. In all the ground states described in Sec. II C these couplings are distributed between the bonds of $\mathcal{T}$ in such a way that in each triangular plaquettes one bond has $K_{jj'} = K_1$, whereas the two other bonds have $K_{jj'} = K_2$.

B. Comparison of different ground states

In the state (e) all sixfold coordinated sites have the identical environment in terms of the coupling constants J_{jk}. As a consequence, the values of the coupling constants $K_{jj'}$ in this state depend only on the orientation of the bonds (jj'). For two of the three possible orientations of the bonds they are equal to each other, see Fig. 4(a). If all sixfold coordinated sites j are renumbered by pairs of integers with the same parity (n, m) as shown in Fig. 5, Eq. (15) in this state can be rewritten as

$$\begin{aligned}[2K_S - \Lambda(\omega)]u_{n,m} = {} & K_1^{(m)}u_{n+1,m+1} + K_2^{(m)}u_{n-1,m+1} \\ & + K_1^{(m-1)}u_{n-1,m-1} + K_2^{(m-1)}u_{n+1,m-1} \\ & + K_2[u_{n+2,m} + u_{n-2,m}],\end{aligned} \tag{19}$$

where $K_S = K_1 + 2K_2$ and

$$K_1^{(m)} = K_1, \quad K_2^{(m)} = K_2, \tag{20}$$

for all values of m.

For $K_{1,2}^{(m)}$ given by Eq. (20), Eq. (19) can be easily solved after performing the Fourrier transformation. Substitution of

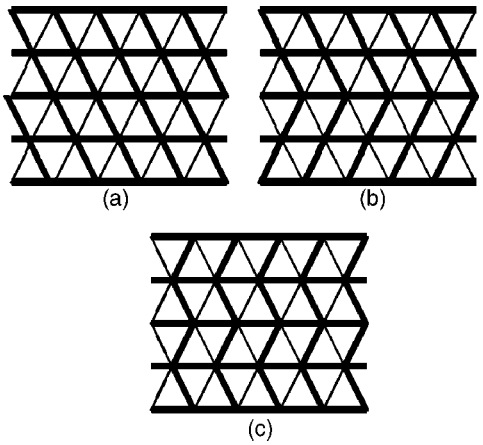

FIG. 4. The distribution of coupling constants $K_{jj'}$ between the bonds of $\mathcal{T}$ in different states: (a) states *a* and *e*; (b) a single type I domain wall; and (c) states *c* and *g*. Thin lines correspond to $K_{jj'} = K_1$ and thick lines to $K_{jj'} = K_2$.

$u_{n,m} \propto \exp i(qn+pm)$ into Eq. (19) gives the dispersion relation in the form

$$\Lambda(\omega) = 2K_S - 2K_1 \cos(q+p) - 2K_2[\cos(q-p) + \cos 2q]. \tag{21}$$

Note that Eq. (21) is of the second order in ω^2, which corresponds to the existence of the two momentum-dependent eigenfrequencies, $\omega_1(q,p)$ and $\omega_2(q,p)$, for each point in the Brillouin zone in addition to $\omega_0=(J_S/M_3)^{1/2}$ discussed above.

According to Eq. (11), each zero-energy domain wall of the type II leads to the permutation of the coupling constants J_1 and J_3 in the Hamiltonian of harmonic fluctuations. Such a permutation does not change the factor $J_S-M_3\omega^2$ in the right-hand side of Eq. (14b), and therefore does not change neither the degeneracy, nor the frequency, ω_0, of the family of the eigenmodes with $u=0$. Since Eqs. (18) are also invariant with respect to the permutation of J_1 and J_3, such a permutation introduces no changes to the form of Eq. (15) as well. This means that the whole set of the eigenfrequencies of the harmonic fluctuations in the system does not feel the presence of the type II domain walls and is exactly the same in all the states which can be obtained from each other by the insertion of the type II domain walls. For example, the dispersion relation (21) is valid not only in the state (e), but also in the state (a), which is characterized by exactly the same pattern of the coupling constants $K_{jj'}$ shown in Fig. 4(a).

The zero-energy domain walls of the type I lead to a more complex permutation of coupling constants. However, in the terms of the coupling constants $K_{jj'}$ the consequences of this permutation are rather simple and reduce to the permutation of K_1 and K_2 for those two orientations of the bonds (jj') that are not parallel to the direction of the wall,[34] see Fig. 4(b). This means that Eqs. (20) should be valid only when d_m, the number of the type I domain walls situated at $m' \leqslant m$, is even and should be replaced by

$$K_1^{(m)} = K_2, \quad K_2^{(m)} = K_1$$

when d_m is odd.

In the presence of periodic boundary conditions in the horizontal direction and open boundary conditions in the perpendicular (vertical) direction the irrelevance of such permutations of coupling constants for the set of eigenfrequencies can be easily demonstrated in the framework of the mixed representation which is obtained after performing the Fourier transformation with respect to the variable n, keeping the variable m as it is. In the terms of the variable $u_m(q)$ defined in such a way, Eq. (19) can be rewritten as

$$[2K_S - \Lambda(\omega)]u_m(q) = K^{(m)}(q)u_{m+1}(q) + 2K_2 \cos(2q)u_m(q) + K^{(m-1)}(q)u_{m-1}(q), \tag{22}$$

where

$$K^{(m)}(q) = K_0(q)\exp[i\alpha(q)s_m].$$

The dependence of $K^{(m)}(q)$ on m enters only through $s_m=(-1)^{d_m}=\pm 1$, whereas both

$$K_0(q) = |K_1 \exp(iq) + K_2 \exp(-iq)|$$

and

$$\alpha(q) = \arg[K_1 \exp(iq) + K_2 \exp(-iq)]$$

are independent of m.

With the help of the simple gauge transformation

$$u_m(q) = \exp\left[i\alpha(q) \sum_{m'<m} s_m \right] u'_m(q), \tag{23}$$

which cannot not change the eigenvalues, Eq. (22) can be transformed to the form

$$[2K_S - \Lambda(\omega)]u'_m(q) = K_0(q)u'_{m+1}(q) + 2K_2 \cos(2q)u'_m(q) + K_0(q)u'_{m-1}(q), \tag{24}$$

in which all coefficients do not depend on m. This property of Eq. (24) proves that for the considered boundary conditions the whole set of eigenfrequencies is insensitive to the presence of domain walls of the type I. Since Eq. (24) has been derived from Eq. (19), the form of which does not depend on the presence of the zero-energy domain walls of the type II, the same conclusion is applicable also in the presence of an intersecting network of zero-energy domain walls of both types.

Note that this does not mean that the spectrum of fluctuations in an infinite system, understood as the dependence of the eigenfrequencies on the two-dimensional wave vector, is the same for all periodic ground states. On the contrary, it should have different forms in the states whose transformation into each other requires the insertion of a periodic sequence of the type I domain walls. In particular, the dispersion relation in the state (c) and state (g) [which can be obtained from each other by the insertion of the dense sequence of type II domain walls and both are characterized by the distribution of the coupling constants $K_{jj'}$ shown in Fig. 4(c)] can be obtained by substitution of $u'_m(q) \propto \exp(ipm)$ into Eq. (24) and is of the form

$$\Lambda(\omega) = 2K_S - 2K_0(q)\cos p - 2K_2 \cos 2q. \tag{25}$$

Apparently, it does not coincide with the dispersion relation in the states (a) and (e) given by Eq. (21). Note that the elementary cell of the state (c) consists of 12 sites, and, therefore, a more straightforward approach to the derivation of its dispersion relation would give it in the form of the determinant of a 12 by 12 matrix.

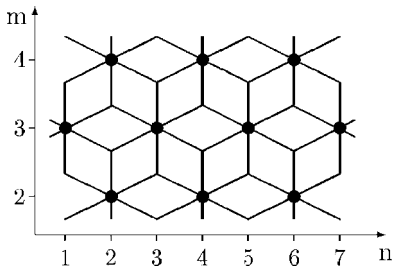

FIG. 5. The numbering of the sixfold coordinated sites by pairs of integers (n,m) with the same parity.

However, the free energy of harmonic fluctuations, F_2, which in a general situation (that is, when the quantum effects are also taken into account) can be written as

$$F_2 = T\sum_{\{\omega\}} \ln\left(2\sinh\frac{\hbar\omega}{2T}\right) \tag{26}$$

is determined entirely by the set of the eigenfrequencies of the system $\{\omega\}$. Thus our results demonstrate that for the considered boundary conditions the value of F_2 is exactly the same for all the ground states discussed above even in the case of a finite system. For other types of boundary conditions the same property will be recovered in the thermodynamic limit.

Naturally, these conclusions should remain valid both in the zero-temperature limit, when Eq. (26) is transformed into the expression for the energy of zero-point fluctuations,

$$E_2 = \frac{\hbar}{2}\int\int\frac{dqdp}{(2\pi)^2}[\omega_0 + \omega_1(q,p) + \omega_2(q,p)],$$

and in the classical limit ($\hbar \to 0$), when the dynamical properties of the system are of no importance, and Eq. (26) is reduced to

$$F_2 = \frac{T}{2}\int\int\frac{dqdp}{(2\pi)^2}\ln\left[\frac{\Lambda(q,p)}{T}\right],$$

where $\Lambda(q,p)$ denotes the function of q and p standing in the right-hand side of the corresponding dispersion relation, Eq. (21) or Eq. (25).

Another system, in which the accidental degeneracy of its ground states remains unbroken when the free energy of the harmonic fluctuations is taken into account, is the fully frustrated XY model with a honeycomb lattice.[16] The method used in this section (the construction of the gauge transformation which reduces the linearized equations of motion for fluctuations in different ground states to the same form) presents a generalization of the approach of Ref. 16, where the analogous gauge transformation has been constructed for the harmonic part of the Hamiltonian.

The analysis of this section can be generalized for the case when the capacitance matrix of a Josephson junction array in addition to the self-capacitances of superconducting islands also takes into account C_1, the capacitances of Josephson junctions forming the array. This will lead to the replacement

$$J_a \to J_a(\omega) \equiv J_a - M_1\omega^2,$$

where $M_1 = (\hbar/2e)^2 C_1$, in all dispersion relations, but will not bring any changes in the qualitative conclusions. It is equally possible to include into consideration an ohmic dissipation of each junction described by a frequency-dependent harmonic contribution to its Euclidean action.

C. Correlation functions

Since the evolution of the variables u_j can be described by Eqs. (15), which contain only coupling constants $K_{jj'}$, but not the original coupling constants J_{jk}, the symmetry of the correlation function of the variables u_j in a given state will be determined entirely by the symmetry of the configuration of $K_{jj'}$ in this state. In particular, in the situation when the value of $K_{jj'}$ depends only on the orientation of the bond (jj') and can be equal only to K_1 or K_2, the correlation function

$$G_{jj'} = \langle (u_j - u_{j'})^2 \rangle, \tag{27}$$

where j and j' are the nearest neighbors of each other on $\mathcal{T}$, should also be dependent only on the orientation of the bond (jj') and acquire one of the two possible values, which below are denoted G_1 and G_2. The same property can be described by saying that in such states $G_{jj'}$ depends only on whether $K_{jj'}$ is equal to K_1 or to K_2,

$$G_{jj'} = \begin{cases} G_1 & \text{for } K_{jj'} = K_1, \\ G_2 & \text{for } K_{jj'} = K_2. \end{cases} \tag{28}$$

The type II domain walls are simply of no consequence for the values of $K_{jj'}$ and, therefore, for the correlation functions of the variables u. On the other hand, it is rather evident that the gauge transformation (23) leaves invariant the form of the correlation functions of the variables $u_{n,m}$ with the same value of m. This means that the correlation function $\langle (u_j - u_{j'})^2 \rangle$ cannot be sensitive to the presence of the type I domain walls which do not pass between the points j and j'. Since the sites j and j', which are the nearest neighbors of each other on $\mathcal{T}$, are too close to have a domain wall passing between them, Eq. (28) will be applicable also in the presence of an arbitrary set of zero-energy domain walls.

IV. ANHARMONIC FLUCTUATIONS

In this section and below our analysis is restricted to the classical version of the model. It is well known that in a classical system the leading contribution to the free energy related to anharmonic fluctuations, $F_{\text{anh}} = F_3 + F_4$, is the sum of the two terms,

$$F_3 = -\frac{1}{2T}\langle [H^{(3)}]^2 \rangle \tag{29}$$

and

$$F_4 = \langle H^{(4)} \rangle, \tag{30}$$

where $H^{(3)}$ and $H^{(4)}$ are, respectively, the third- and the forth-order contributions to the expansion of the Hamiltonian in the vicinity of a particular ground state, and angular brackets denote the averages over thermodynamic fluctuations calculated with the help of the harmonic Hamiltonian.

In the considered problem $H^{(3)}$ and $H^{(4)}$ can be written as

$$H^{(3)} = \sum_k H_k^{(3)}; \quad H_k^{(3)} = -\frac{1}{6}\sum_{j=j(k)} J'_{jk}(u_j - v_k)^3$$

and

$$H^{(4)} = \sum_k H_k^{(4)}; \quad H_k^{(4)} = -\frac{1}{24}\sum_{j=j(k)} J_{jk}(u_j - v_k)^4,$$

where coupling constants J_{jk} are exactly the same as in the harmonic Hamiltonian, Eq. (12), whereas coupling constants $J'_{jk}=J\sin\theta_{jk}$ acquire one of the six possible values $J'_{jk}=\pm J\sin\theta_a$ in accordance with the value of θ_{jk} on the bond (jk). Due to the current conservation condition coupling constants J'_{jk} have to satisfy the constraints,

$$\sum_{j=j(k)} J'_{jk} = 0, \quad \sum_{k=k(j)} J'_{jk} = 0, \tag{31}$$

on all sites of the lattice.

A. Invariance of F_4

In the case of a dice lattice there exists a convenient way to separate the fluctuations on the two types of sites from each other, which allows one to considerably simplify the calculation of the averages in Eqs. (29) and (30). It consists of the replacement of variables

$$v_k = w_k + v_k^{(0)}, \quad v_k^{(0)} = \sum_{j=j(k)} J_{jk}u_j/J_S, \tag{32}$$

which transforms the harmonic Hamiltonian (12) into

$$H^{(2)} = \frac{1}{2}\sum_{(jj')} K_{jj'}(u_j - u_{j'})^2 + \frac{1}{2}\sum_k J_S w_k^2, \tag{33}$$

where the coupling constants $K_{jj'}$ are, naturally, the same as have been obtained in Sec. III B, see Eqs. (17) and (18), after the exclusion of the variables v_k from the equations of motion.

A simple form of Eq. (33), in which each variable w_k is decoupled from all other variables, makes the calculation of averages with respect to the fluctuations of w_k a very straightforward procedure. Substitution of Eq. (32) into the expression for $H_k^{(4)}$ with subsequent expansion of the result in powers of w_k allows one to express the result of such an averaging of $H_k^{(4)}$ as a fourth-order polynomial of the variables u_j,

$$P_4(u_{j_1},u_{j_2},u_{j_3}) = -\frac{1}{24}\sum_{a=1}^{3} J_a(3\langle w^2\rangle^2 + 6\langle w^2\rangle\tilde{u}_{j_a}^2 + \tilde{u}_{j_a}^4), \tag{34}$$

where $\langle w^2\rangle = T/J_S$ is the value of $\langle w_k\rangle^2$, which is the same for all k, whereas

$$\tilde{u}_{j_a} \equiv u_{j_a} - v_k^{(0)} = \frac{1}{J_S}\sum_{b\neq a} J_b(u_{j_a} - u_{j_b}).$$

All terms which are odd in w_k have disappeared from Eq. (34) due to the corresponding symmetry of the Hamiltonian (33). Note that the form of $P_4(u_1,u_2,u_3)$ does not depend on k. To achieve that we have renumbered in Eq. (34) the three sites j which are the nearest neighbors of k as $j_a \equiv j_a(k)$ in such a way that $J_{j_a k}=J_a$.

Since Hamiltonian (33) does not include linear terms, the result of the Gaussian averaging of $P_4(u_{j_1},u_{j_2},u_{j_3})$ will have the form of a second-order polynomial, $P_2(G_{j_1j_2},G_{j_2j_3},G_{j_1j_3})$, whose three arguments are the nearest-neighbor correlation functions defined by Eq. (27). Instead of looking for the explicit form of P_2, it is sufficient to notice that since the central vortex of a triad is always surrounded by the bonds with J_{jk} equal to J_1 or J_3, we will always have $K_{j_1j_3}=K_1$ and $K_{j_1j_2}=K_{j_2j_3}=K_2$, and, as a consequence of Eq. (28), the result of the averaging of $H^{(4)}$ will have the same form,

$$\langle H_k^{(4)}\rangle = P_2(G_2,G_2,G_1),$$

for all k independently of what particular ground state is considered. Therefore the value of $F_4=\Sigma_k\langle H_k^{(4)}\rangle$ will be exactly the same for all the ground states which we are trying to compare already at the level of the separate terms in this sum.

B. Simplification of F_3

The result of the averaging of $H_k^{(3)}$ with respect to fluctuations of w_k can be in an analogous way reduced to the sum of two terms, the first of which,

$$P_1(u_{j_1},u_{j_2},u_{j_3}) = -\frac{\langle w^2\rangle}{2}\sum_{a=1}^{3} J'_{j_a k}\tilde{u}_{j_a},$$

is a first-order and the second,

$$P_3(u_{j_1},u_{j_2},u_{j_3}) = -\frac{1}{6}\sum_{a=1}^{3} J'_{j_a k}\tilde{u}_{j_a}^3,$$

a third-order polynomial of the variables u_{j_a}, which are assumed here to be numbered in the same way as in Eq. (34). Both P_1 and P_3 depend on k only through the factor $\tau_k=\pm 1$, which, for example, can be chosen to be determined by the sign of $J'_{j_1 k}$.

The sum of $P_1(u_{j_1},u_{j_2},u_{j_3})$ over k can be reordered as a sum over j,

$$\sum_k P_1(u_{j_1},u_{j_2},u_{j_3})|_k = -\frac{\langle w^2\rangle}{2J_S}\sum_j C_j u_j,$$

where

$$C_j = \sum_{k=k(j)} [J'_{jk}(J_{j'k} + J_{j''k}) - J_{jk}(J'_{j'k} + J'_{j''k})]$$

and j' and j'' are the other two nearest neighbors of k in addition to j. It is not hard to notice that all coefficients C_j are equal to zero as a consequence of Eqs. (31).

This allows one to express the result of the averaging of $[H^{(3)}]^2$ over fluctuations of the variables w_k as

$$\langle [H^{(3)}]^2\rangle_w = R^2 + \sum_k P_6(u_{j_1},u_{j_2},u_{j_3}) \tag{35}$$

where

$$R = \sum_k P_3(u_{j_1},u_{j_2},u_{j_3}) \tag{36}$$

and P_6 is a sixth-order polynomial of its arguments, the form of which is the same for all k. Exactly like it happens with

P_4, the averaging of $P_6(u_{j_1},u_{j_2},u_{j_3})$ over fluctuations of u_j produces the same expression for all k independently of what particular ground state is considered. That means that any difference between the values of $F_{\rm anh}$ in different ground states can result only from the first term in Eq. (35),

$$F_{\rm anh} = {\rm const} - \frac{1}{2T}\langle R^2\rangle. \tag{37}$$

C. Explicit expressions

Let us start with comparing the free energies of anharmonic fluctuations in the states (a) and (e). Instead of calculating $F_{\rm anh}$ separately for both these states it is more convenient to construct an explicit expression directly for $\delta F^{\rm e,a}_{\rm anh}=F^{\rm e}_{\rm anh}-F^{\rm a}_{\rm anh}$, the difference in $F_{\rm anh}$ between the states (e) and (a). Since both these states are characterized by the same form of the effective Hamiltonian for the variables u_j, the construction of such an expression does not require the application of the gauge transformation given by Eq. (23). The same is true also for the whole set of states which can be constructed from the state (a) or state (e) by the insertion of some sequence of type II domain walls.

If the state (e) shown in Fig. 3(e) is rotated by $\pi/3$ in such a way that the orientation of the possible type II domain walls becomes horizontal, the expression for R, Eq. (36), in this state can be rewritten as

$$R^{\rm e} = \sum_m \sigma_m S^+_m, \tag{38}$$

where we have again used the numbering of sites defined by Fig. 5, $\sigma_m=(-1)^m$,

$$S^\mu_m = \sum_{n=m({\rm mod}\ 2)} [P^\mu_3(u_{n+2,m},u_{n+1,m+1},u_{n,m}) + P^\mu_3(u_{n+1,m+1},u_{n,m},u_{n-1,m+1})], \tag{39}$$

and $P^+_3=\tau_k P_3$ is an invariant version of P_3,

$$P^+_3(u_1,u_2,u_3) = -\frac{1}{6J^3_S}\sum_{a=1}^{3} J'_a\left[\sum_{b\neq a} J_b(u_a-u_b)\right]^3, \tag{40}$$

the form of which does not depend on k. Instead of introducing a definition simply for S^+_m, we have used Eq. (39) to define a more general object S^μ_m, where superscript μ can be equal to ±1 or 0. However, for the compactness of notation we will usually replace $\mu=\pm1$ simply by plus or minus. In Eq. (40) the constants J'_{jk} are expressed in terms of three constants,

$$J'_1 = J\sin\theta_1 = \left(\frac{1}{\sqrt{3}}-\frac{1}{\sqrt{6}}\right)J, \tag{41a}$$

$$J'_2 = J\sin\theta_2 = \frac{2}{\sqrt{6}}J, \tag{41b}$$

$$J'_3 = -J\sin\theta_3 = -\left(\frac{1}{\sqrt{3}}+\frac{1}{\sqrt{6}}\right)J, \tag{41c}$$

whose sum is equal to zero in accordance with Eqs. (31).

Substitution of Eqs. (13) and (41) into Eq. (40) allows one to reduce it to

$$P^+_3(u_1,u_2,u_3) = K_3(u_2-u_3)^2(u_3-u_1) + K'_3(u_1-u_2)^3 + K''_3(u_3-u_1)^3, \tag{42}$$

where

$$K_3 = \frac{J}{6\sqrt{6}},\quad K'_3 = \frac{J}{9\sqrt{6}},\quad K''_3 = \left(\frac{1}{9\sqrt{3}}-\frac{1}{36\sqrt{6}}\right)J.$$

However, in all the ground states that we consider the last term from Eq. (42) after substitution of $P_3=\tau_k P^+_3$ into Eq. (36) cancels with the analogous term from the neighboring triangular plaquette, which allows one to put $K''_3=0$.

Each time a type II domain wall is crossed the replacement of variables θ_j described by Eqs. (11) has to take place. In terms of the expression for R this procedure is translated into the replacement of each term of the form $P^+_3(u_1,u_2,u_3)$ by

$$P^-_3(u_1,u_2,u_3) = -P^+_3(u_3,u_2,u_1).$$

As a consequence, the value of R for the state which is obtained after the insertion of the dense sequence of type II domain walls [the structure of this state is obtained after rotating Fig. 3(a) by $\pi/3$] will have the form

$$R^{\rm a} = \sum_m \sigma_m S^{\sigma_m}_m. \tag{43}$$

Substitution of Eqs. (38) and (43) into Eq. (37) allows one to express $\delta F^{\rm e,a}_{\rm anh}$ as

$$\delta F^{\rm e,a}_{\rm anh} = N\sum_{l=1}^{\infty} V(2l-1), \tag{44}$$

where $V(m)$ is the average

$$V(m) = \frac{2}{TL_x}\langle S^0_{m_1}S^0_{m_2}\rangle, \tag{45}$$

which depends only on $m=m_1-m_2$, L_x is the size of the system in the horizontal direction (in lattice unites of $\mathcal{T}$) and S^0_m is given by Eq. (39) with

$$P^0_3(u_1,u_2,u_3) = \frac{1}{2}[P^+_3(u_1,u_2,u_3) - P^-_3(u_1,u_2,u_3)] = \frac{1}{2}[P^+_3(u_1,u_2,u_3) + P^+_3(u_3,u_2,u_1)]$$

being the symmetric (with respect to the permutation of u_1 and u_3) part of $P^+_3(u_1,u_2,u_3)$. The explicit expression for $P^0_3(u_1,u_2,u_3)$ which follows from Eq. (42) is

$$P^0_3(u_1,u_2,u_3) = \frac{K_3}{2}(u_3-u_1)^2(u_3-2u_2+u_1) + \frac{K'_3}{2}[(u_1-u_2)^3+(u_3-u_2)^3]. \tag{46}$$

Analogous comparison of the values of $F_{\rm anh}$ in two different states allows one to find that the free energy of a single

type II domain wall on the background of the state (a) is given by

$$F_{\mathrm{DW}} = L_x \sum_{m=1}^{\infty} mV(m), \tag{47}$$

whereas the interaction of two domain walls situated at $m=m_1$ and $m=m_2$ can be written as

$$F_{\mathrm{int}}(m_2 - m_1) = -2L_x \sum_{m=1}^{\infty} mV(|m_2 - m_1| + m). \tag{48}$$

D. Continuous approximation

When Eq. (46) is substituted in the expression for S_m^0 given by Eq. (39) with $\mu=0$, all terms proportional to K_3' cancel each other after the summation over n, so it becomes possible to rewrite this expression as

$$S_m^0 = 4K_3 \Bigg[\sum_{n=m'(\mathrm{mod}\ 2)} (\nabla_n u)^2 (\nabla_{m'}^{+} u)|_{m'=m+1} - \sum_{n=m'(\mathrm{mod}\ 2)} (\nabla_n u)^2 (\nabla_{m'}^{-} u)|_{m'=m} \Bigg], \tag{49}$$

where

$$\nabla_n u \equiv \frac{u_{n+2,m'} - u_{n,m'}}{2}$$

is a lattice analog of the derivative in the horizontal direction and

$$\nabla_{m'}^{\pm} u \equiv \pm \left[\frac{u_{n,m'} + u_{n+2,m'}}{2} - u_{n+1,m'\mp 1} \right]$$

are two lattice analogs of the derivative in the vertical direction suitable for a triangular lattice. It follows from symmetry reasons that

$$\langle (\nabla_n u)(\nabla_m^{\pm} u) \rangle = 0. \tag{50}$$

The function S_m^0 defined by Eq. (49) is a third-order polynomial of variables $u_{n,m'}$ belonging to the stripe with $m'=m, m+1$. Accordingly, the result of the Gaussian averaging of the product $S_{m_1}^0 S_{m_2}^0$ will be a third-order polynomial of the two-point correlation functions. It is not hard to check that the only terms which survive in the expression for $\langle S_{m_1}^0 S_{m_2}^0 \rangle$ are the triple products of the two-point correlation functions whose arguments belong to different stripes, whereas all other terms cancel each other in the result of the summation over n or as a consequence of Eq. (50). Speaking more precisely, due to the structure of the expression for S_m^0, Eq. (49), they are the triple products of the lattice analogs of the derivatives of such correlation functions, which for $|m_1 - m_2| \gg 1$ can be rather accurately calculated in the framework of the continuous approximation.

When integer variables n and m are replaced by continuous variables x and y, both the first and the second term in the square brackets in Eq. (49) should be replaced by the same integral

$$\frac{1}{2} \int dx u_x^2 u_y,$$

where, however, u_x^2 should be calculated at the values of y which differ from each other by one (in this section subscripts x and y designate partial derivatives with respect to the corresponding variables). This means that in the framework of the continuous approximation the total expression for S_m^0 should be replaced by

$$(S_m^0)_{\mathrm{cont}} = \sqrt{2} K_3 \int dx (u_x^2)_y u_y = -\sqrt{2} K_3 \int dx u_{xx} u_y^2. \tag{51}$$

When writing Eq. (51) we have performed the integration by parts and also the rescaling $x \to \lambda x$ ($\lambda^2 = 1 + 2K_1/K_2 = 2$), which transforms the continuous version,

$$H_{\mathrm{cont}}^{(2)} = \frac{1}{2} \int \int dx dy [(2K_1 + K_2) u_x^2 + K_2 u_y^2],$$

of the harmonic Hamiltonian,

$$H^{(2)} = \sum_{n=m(\mathrm{mod}\ 2)} \sum_m \left[\frac{K_1}{2} (u_{n+2,m} - u_{n,m})^2 + \frac{K_2}{2} \sum_{l=\pm 1} (u_{n+1,m+l} - u_{n,m})^2 \right],$$

to the isotropic form,

$$H_{\mathrm{isotr}}^{(2)} = \frac{K_{\mathrm{eff}}}{2} \int \int dx dy [u_x^2 + u_y^2], \tag{52}$$

where

$$K_{\mathrm{eff}} = \sqrt{(2K_1 + K_2) K_2} = \left(\frac{2}{3} \right)^{3/2} J.$$

Substitution of the correlation function,

$$G(x,y) = \mathrm{const} - \frac{T}{2\pi K_{\mathrm{eff}}} \ln (x^2 + y^2)^{1/2},$$

corresponding to the Hamiltonian (52) into

$$\langle (S_{m_1}^0)_{\mathrm{cont}} (S_{m_2}^0)_{\mathrm{cont}} \rangle = 2K_3^2 \int_{-\infty}^{\infty} dx_1 \int_{-\infty}^{\infty} dx_2 [2G_{xxxx} G_{yy}^2 + 4G_{xxy}^2 G_{yy}],$$

[where all derivatives of $G(x,y)$ should be taken at $x=x_1 - x_2$, $y=y_1 - y_2$] and subsequent integration over $x_1 - x_2$ give

$$V_{\mathrm{cont}}(m) = \gamma_c \frac{T^2}{J} \frac{1}{|m_1 - m_2|^7}, \tag{53}$$

where

$$\gamma_c = 2\sqrt{2} \frac{2K_3^2 J}{(2\pi K_{\mathrm{eff}})^3} \frac{15\pi}{4} = \frac{45\sqrt{3}}{1024\pi^2} \approx 0.0077.$$

Thus we have found that the quantity $V(m)$, the summation of which over m allows one to find different essential free energies, contains a very small numerical coefficient γ_c

and very rapidly decays with the increase of m. Accordingly, the expressions in Eqs. (44) and (47) which include the summation of $V(m)$ starting from $m=1$ will be determined entirely by the first term in the sum. However, substitution of Eq. (53) into Eq. (48) with subsequent replacement of the summation by integration allows one to find the form of the interaction of two domain walls for $m \gg 1$,

$$F_{\rm int}(m) \approx -\frac{\gamma_c}{15}\frac{T^2}{J}\frac{L_x}{m^5}.$$

E. Numerical calculations

Note that the expression for $V(m)$, Eq. (53), which we have found in the framework of the continuous approximation is positive and increases with decrease of m, that is when one moves out of the region of the applicability of the continuous approximation. Although it hardly can be expected that the more accurate calculation will lead to the change of the sign of $V(m)$, we have checked this for $m=1$ by going beyond the limits of the continuous approximation.

The exact expression for $V(m)$ given by Eqs. (45) and (49) can be written as a sum over all possible pairs of triangles belonging to two different stripes. For $m=1$ the first term in this sum, that is the contribution which corresponds to the pair of adjacent triangles, has the form

$$V_0(1) = \frac{4K_3^2}{T}\langle (u_{n+2,m}-u_{n,m})^2\rangle^2 \langle (\nabla_m^+ u)(-\nabla_m^- u)\rangle. \quad (54)$$

The averages which enter Eq. (54) are given by the integrals over Brillouin zone,

$$\langle (u_{n+2,m}-u_{n,m})^2\rangle = \int_{-\pi}^{\pi}\int_{-\pi}^{\pi}\frac{dqdp}{(2\pi)^2}\frac{W_1(q,p)T}{\Lambda_0(q,p)},$$

$$\langle (\nabla_m^+ u)(-\nabla_m^- u)\rangle = \int_{-\pi}^{\pi}\int_{-\pi}^{\pi}\frac{dqdp}{(2\pi)^2}\frac{W_2(q,p)T}{\Lambda_0(q,p)},$$

where

$$W_1(q,p) = 2(1-\cos 2q),$$

$$W_2(q,p) = (\cos q - \cos p)^2 - \sin^2 p,$$

$$\Lambda_0(q,p) = 2K_1(1-\cos 2q) + 4K_2(1-\cos q \cos p).$$

Numerical calculation of these integrals gives

$$\langle (u_{n+2,m}-u_{n,m})^2\rangle \approx 0.433\frac{T}{K_2},$$

$$\langle (\nabla_m^+ u)(-\nabla_m^- u)\rangle \approx 0.0294\frac{T}{K_2},$$

which after substitution into Eq. (54) allows one to find that $V_0(1)=\gamma_0 T^2/J$, where $\gamma_0 \approx 0.0018$.

The addition to Eq. (54) of the analogous terms related to the pairs of triangular plaquettes which have a common site leads to the replacement of γ_0 by $\gamma_2 \approx 0.0032 > 0$. The contributions from more distant pairs of plaquettes are much smaller and can be safely neglected. This result confirms the positiveness of $V(1)$. According to Eq. (44), the positiveness of $V(m)$ for all m ensures that $F_{\rm anh}^{\rm e} > F_{\rm anh}^{\rm a}$.

It follows from Eq. (47) that the value of the type II domain wall free energy per unit length can be then rather accurately estimated as

$$f_{\rm DW}^{(0)} = \gamma_2 \frac{T^2}{J}. \quad (55)$$

In the analysis of the next section $f_{\rm DW}^{(0)}(T)$ plays the role of the fluctuation-induced effective energy of a domain wall.

The comparison of the free energies of anharmonic fluctuations in the states (a) and (c) can be made following the same approach, but turns out to be much more cumbersome for two reasons. First, in order to reduce the Hamiltonians of the harmonic fluctuations in these two states to the same form one has to apply the gauge transformation introduced in Sec. III B. Second, there is no complete cancellation of the second term from Eq. (42), which leads to the strong increase of the number of terms one has to take into account in the expressions for the free energies of fluctuations. A numerical calculation shows that the free energy of anharmonic fluctuations is lower for the state (a), which means that the free energy of the type I domain wall shown in Fig. 3(b) is also positive.

The numerical constant γ_1 characterizing this free energy is equal to 0.0044 if one takes into account only the contributions from the adjacent plaquettes, whereas when the contributions from the pairs of plaquettes which have a common site are also included, one gets the value which is very close to γ_2,

$$\gamma_1 \approx 0.0033.$$

V. DISORDERING OF VORTEX PATTERN

A. An estimate for the phase transition temperature

The temperature of the phase transition associated with the proliferation of domain walls and the disordering of the periodic vortex pattern can be estimated by analyzing a more complete expression for the domain wall free energy, which in addition to the term induced by anharmonicities, $f_{\rm DW}^{(0)}(T)=\gamma T^2/J$, should also include the entropic term related to the formation of kinks,

$$f_{\rm DW}(T) = f_{\rm DW}^{(0)}(T) - \nu T \exp(-E_{\rm K}/T),$$

where $E_{\rm K} \propto J$ is the energy of a kink and $\nu \sim 1$ is the density (per unit length) of the positions on a domain wall where a kink can exist. In the case of the exactly solvable anisotropic Ising model[35] an analogous estimate allows one to find the transition temperature with the exponential accuracy.

The temperature of the phase transition associated with the spontaneous creation of infinite domain walls, T_c, can be then estimated from the condition $f_{\rm DW}(T_c)=0$, which can be rewritten as

$$T_c = \frac{E_K}{\ln[\nu T_c / f_{DW}^{(0)}(T_c)]}. \quad (56)$$

Equation (56) shows that T_c is determined mainly by E_K and only logarithmically depends on $f_{DW}^{(0)}$, that is on γ.

Figure 6(a) shows the structure of an elementary kink on a type I domain wall separating two different versions of the state (a). This is one of the simplest neutral pointlike excitations possible in the system. It contains only two vortex clusters of anomalous sizes, one with four positive vortices (instead of three) and another with two, so there is no excess vorticity associated with this defect. Note that any defect with only one vortex cluster of anomalous size will be characterized by a nonzero vorticity, so its energy will be logarithmically divergent.

The distance between two neighboring positions the kink shown in Fig. 6(a) can occupy is equal to 2 (in lattice units of $\mathcal{T}$). However, the same domain wall allows also for the formation of kinks of the opposite sign (orientation), which means that the value of ν in Eq. (56) should be set equal to one.

Numerical calculation of the kink energy has been performed by minimizing the energy of a finite lattice cluster around the kink (with the size $4L \times 4L$, containing $N = 48L^2 - 10L + 1$ sites inside it) with the assumption that on all sites outside of this area the values of the phases are exactly the same as they would be if the kink was infinitely far. Numerical calculation of E_K for $L = 1, 2, 3$ ($L = 3$ corresponds to $N = 403$) and extrapolation of the result to $L \to \infty$ give

$$\frac{E_K}{J} = 0.1037 \pm 0.0001. \quad (57)$$

The simplest kink on a type II domain wall is also neutral, but has a more complex structure. It contains four vortex clusters of anomalous sizes, and, therefore, its energy is, roughly speaking, two times larger then the energy of a kink on a type I domain wall. This means that in the vicinity of the phase transition type I domain walls play a relatively more important role. Numerical solution of Eq. (56) for $E_K/J = 0.1037$ and $\gamma = 0.0033$ gives

$$T_c/J \approx 0.010. \quad (58)$$

B. Vortex pattern fluctuations in the low temperature phase

At $T < T_c$ all domain walls excited as thermal fluctuations should have the form of closed loops. At temperatures well below T_c the form of these loops will be strongly anisotropic. At $T \ll T_c$ a typical defect will be formed by two parallel zero-energy domain walls separated by the minimal possible distance.[22] Accordingly, the free energy of such a stripe defect can be written as

$$F_{SD}(L,T) = 2E_0 + 2f_{DW}^{(0)}(T)L,$$

where E_0 is the energy which can be associated with each of the two ends of stripe defect and L is its length. Since in the considered problem the structure of the end point of a striped defect is the same as the one of the kink [see Fig. 6(b)], E_0 is very close to E_K.

The probability of formation of stripe defects, $P_{SD}(L)$, is, naturally, determined by their free energies,

$$P_{SD}(L) = \exp[-F_{SD}(L)/T],$$

which allows one to estimate ρ, the fraction of the total area of the system covered by such defects, as

$$\rho(T) \sim \left[\frac{T}{f_{DW}^{(0)}(T)}\right]^2 \exp\left(-\frac{2E_0}{T}\right). \quad (59)$$

By looking when $\rho(T)$ becomes of the order of 1, a criterium is obtained which differs from Eq. (56) only by the replacement $E_K \to E_0$. Since $E_0 \approx E_K$, this gives an additional support for our estimate of the phase transition temperature.

However, in this approach it becomes more clear that the estimate we have constructed is an estimate from below. Since stripe defects are strongly anisotropic and can have different orientations, they have to start crossing each other

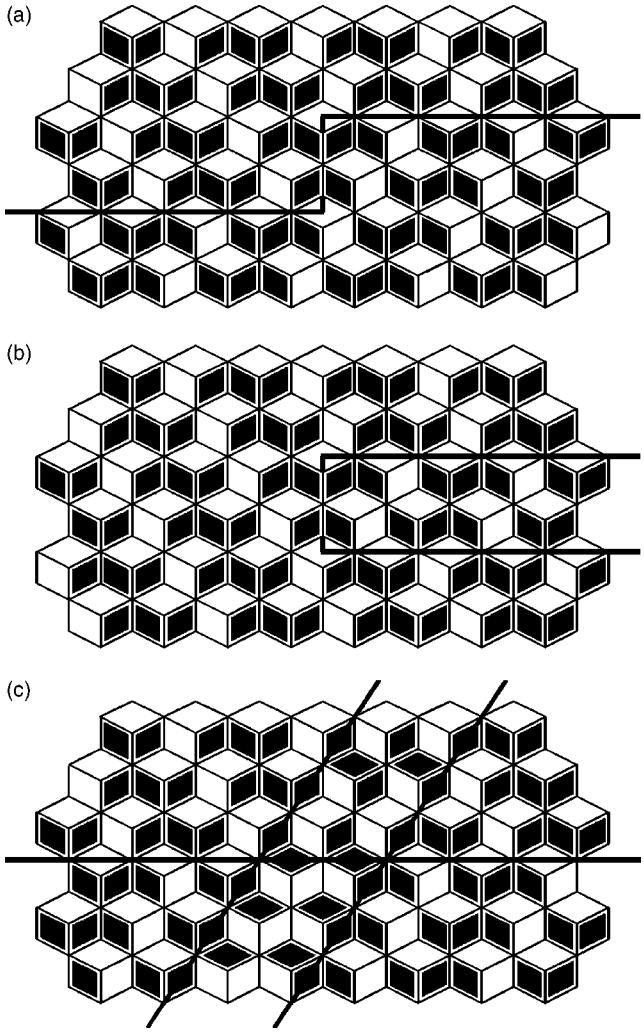

FIG. 6. Pointlike defects with finite energies: (a) a kink on a type I domain wall, (b) an end point of a striped defect with the minimal width, and (c) an intersection of a striped defect with a type I domain wall.

while ρ is still much smaller than 1. An estimate shows that the average distance between the centers of stripe defects becomes comparable with their average length when $T \approx \frac{2}{3} T_c$. Since each of such crossings costs an additional energy, this will decrease the rate at which $\rho(T)$ grows with increasing temperature [as well as the rate at which $f_{\mathrm{DW}}(T)$ decreases].

The defect which is formed when a stripe defect crosses a type I domain wall with different orientation is shown in Fig. 6(c). Like the two other types of local defects considered above this defect is neutral and consists of two clusters of anomalous sizes (four and two), which suggests that its energy is also close to E_{K}. Since no additional energy scale is involved, one can hope that the effects related with such crossings will lead only to the appearance of some numerical factor (comparable with 1) in the right-hand side of Eq. (56).

Note that one also cannot exclude a possibility that the disordering of the vortex pattern is a multistage process and takes place as a sequence of phase transition, the first of which, at $T_c \sim 0.01J$, is related to the appearance of infinite domain walls with only one orientation.

At $T \to 0$ the value of ρ given by Eq. (59) exponentially tends to zero, which means that with the decrease of temperature the system becomes more and more ordered. Quite remarkably, this is accompanied by the divergence of the correlation radius of fluctuations,

$$r_c(T) \approx \frac{T}{2 f_{\mathrm{DW}}(T)}, \tag{60}$$

which is determined by the average length of the defect. In the low temperature limit $r_c(T) \propto 1/T$.

C. Finite-size effects

Thus we have found that T_c, the temperature of vortex-pattern ordering in the fully frustrated *XY* model on a dice lattice, can be expected to be of the order of $0.01J$. It has to be emphasized that at $T \lesssim T_c$ the fluctuation-induced free energy of domain walls is extremely weak, $f_{\mathrm{DW}}^{(0)} \lesssim 10^{-4} \gamma J$, where $\gamma \ll 0.01$ is an additional small parameter calculated in Sec. IV E.

The very low value of the ratio $f_{\mathrm{DW}}^{(0)}/T$ at $T \lesssim T_c$ leads to the unusual prominence of the finite-size effects consisting of the spontaneous formation of domain walls crossing the whole system. If a sample has a form of a stripe with a finite width, L, the probability (per unit length) to have a domain wall crossing the whole system can be estimated as

$$p(L) \sim \exp\left[-\frac{f_{\mathrm{DW}}(T)}{T} L \right] = \exp\left[-\frac{L}{2 r_c(T)} \right].$$

Vortex-pattern ordering, or, at least, any traces of such an ordering can be expected to be observable only when the average distance between such walls, $r(L) = 1/p(L)$ [for $L \lesssim r_c(T)$ this quantity plays the role of the effective correlation radius induced by the finite-size effects] is much larger then 1, which requires one to have $L \gg r_c(T)$.

In typical systems with discrete degrees of freedom analyzed in statistical mechanics (the simplest example being the isotropic Ising model) a twofold or a threefold decrease of temperature with respect to T_c is usually sufficient to obtain $r_c \sim 1$, which allows one to observe the ordering even in relatively small systems. However, in situations when a finite free energy of domain walls arises only from the anharmonic fluctuations, $r_c(T)$ diverges not only when $T \to T_c$, but also when $T \to 0$,[36] and, therefore, the best conditions for the observation of vortex-pattern ordering in a finite system are achieved at intermediate temperatures. The differentiation of $f_{\mathrm{DW}}(T)/T$ with respect to T shows that the minimum of $r_c(T)$ defined by Eq. (60) is achieved when

$$T = \frac{E_{\mathrm{K}}}{\ln[\nu E_{\mathrm{K}}/f_{\mathrm{DW}}^{(0)}(T)]}. \tag{61}$$

The numerical solution of Eq. (61) for the same values of E_{K} and γ, and substitution of the result into Eq. (60), show that the minimal value of r_c is achieved when $T \approx 0.8 T_c$ and is of the order of 2×10^4. Thus the observation of vortex-pattern ordering requires the linear size of the system to be at least comparable with 10^5.

Note that the finite-size effects discussed in this section are related to the destruction of a genuine long-range order and, therefore, have nothing to do with much more subtle "intrinsic finite-size effects" in a finite system with irrational frustration discussed in Ref. 44.

VI. DESTRUCTION OF PHASE COHERENCE

Up to now we have discussed only one phase transition related to the disordering of the vortex pattern and the proliferation of domain walls. However, the ground states of uniformly frustrated *XY* models are characterized by a combination of discrete and continuous degeneracies, which provides possibilities for the existence of (at least) two different phase transitions.[3] The second phase transition is related to the vanishing of the helicity modulus, $\Gamma(T)$, describing the rigidity of the system with respect to a phase twist. In terms of a Josephson junction array this phase transition corresponds to the destruction of superconductivity. It takes place not necessarily at the same temperature as the vortex-pattern disordering.

The interaction between the discrete and continuous degrees of freedom in uniformly frustrated *XY* models has a nonperturbative nature and is related to the formation of fractional vortices at corners and intersections of domain walls.[7–9] According to the general scheme proposed in Ref. 9, three scenarios are possible in a situation when the disordering of a vortex pattern takes place as a single phase transition (whose temperature we denote T_c) and not as a sequence of phase transitions.[37]

First, the vanishing of the helicity modulus can take place at $T < T_c$, if T_{V}, the temperature of pair dissociation for ordinary (integer) vortices, is lower than T_c. The phase transition at $T = T_{\mathrm{V}}$ in that case has exactly the same nature as the Berezinskii-Kosterlitz-Thouless transition[39] in the conventional *XY* model (without frustration). Numerical simulations,[5,11] as well as analysis of the mutual influence between vortices and kinks on domain walls,[14] demonstrate

that this scenario is realized in the fully frustrated *XY* models on square and triangular lattices.

The vanishing of the helicity modulus can also take place at $T>T_c$, but only if at $T=T_c$ the logarithmical interaction of fractional vortices is strong enough to keep them bound in pairs. Note that at $T<T_c$ the confinement of fractional vortices is ensured by their linear interaction related to a finite free energy (per unit length) of the domain walls which are connecting them. In such a case the loss of phase coherence is related to the dissociation of pairs of logarithmically interacting fractional vortices and can be expected to take place at $T=T_{\mathrm{FV}}>T_c$, where T_{FV} is the solution of the equation,

$$T=\frac{\pi}{2}Q^2\Gamma(T), \tag{62}$$

and $Q<1$ is the topological charge of the elementary fractional vortex. Equation (62) is nothing else but the generalization of the Nelson-Kosterlitz universal relation[40] for fractional vortices.[9] This scenario is realized in the antiferromagnetic *XY* model on a *kagome* lattice, where T_c is expected to be anomalously small, $T_c/J\sim 10^{-4}$,[36] and also in the uniformly frustrated *XY* model with $f=1/3$ on a dice lattice, in which the vortex pattern is disordered at any finite temperature and becomes quasiordered only at $T=0$.[41]

The two transitions can be expected to coincide if at $T=T_c$ the value of $\Gamma(T)$ is sufficiently large to ensure that integer vortices are bound in pairs, but is not large enough to prevent from dissociation the pairs of fractional vortices. In such a case $\Gamma(T)$ jumps to zero exactly at $T=T_c$, the ratio $T/\Gamma(T)$ at the transition point is not universal[9] $[(\pi/2)Q^2<T/\Gamma(T)<\pi/2]$, and the transition is likely to be of the first order.[8,42] The results of numerical simulations suggest that this scenario is quite possibly realized on square lattice at $f=2/5$,[43] as well as at $f=1/8$ and $f=1/10$.[42]

In the case of the fully frustrated *XY* model on a dice lattice the effective value of the helicity modulus (properly averaged over angles) at $T=0$ is $\Gamma_0=(2/3)^{3/2}J\approx 0.54J$, and, therefore, at $T=T_c\ll J$ the integer vortices are strongly bound in pairs. It has been already mentioned in Sec. V that the kinks on both types of zero-energy domain walls [on the background of state (a)] are neutral. Therefore the mechanism which forces T_{V} to be lower than T_c in the fully frustrated models on square and triangular lattices[14] here most probably does not work.

In the considered model the fractional vortices appear at points where two type I zero-energy domain walls cross each other. Figure 7 shows an example of such a crossing. Note that after crossing one of the walls has to be transformed into a type II domain wall. The energy of this state is above the ground state energy because one of the vortex clusters contains only two positive vortices instead of three. The accurate summation of the nominal values of the variables θ_{jk} along a closed loop going around this cluster demonstrates the misfit of $\pi/4$ with respect to what one could expect from counting the number of positive and negative half-vortices inside this loop. The value of the misfit is the same for all closed loops surrounding the anomalous cluster and should be compensated by a continuous rotation of the phase by the same angle in the opposite direction. This means that the cluster consisting of two positive vortices behaves itself as a fractional vortex whose topological charge is equal to $-1/8$.

One also can construct an analogous intersection where one of the clusters is formed by four positive vortices instead of three. The topological charge of such a defect will be equal to $+1/8$. It is clear that when the cluster of an anomalous size consists of negative vortices (instead of positive), the sign of the topological charge is reversed. The topological charges of more complex intersections (containing, for example, the clusters of five or more vortices or several clusters of anomalous sizes) will all be multiples of $1/8$. Note that the excess vorticity which can be associated with a vortex cluster depends not only on its size but also on the shape. For example, when a cluster consists of three vortices, but has the shape of a hexagon, the topological charge which has to be associated with it is equal to $\pm 3/8$.

The only possibility to have domain walls crossings in an equilibrium infinite system well below the temperature of vortex-pattern ordering is related to crossing of stripe defects discussed in Sec. V B. Figure 6(c) shows an example of the intersection of a stripe defect with a domain wall where the two fractional vortices have the opposite topological charges, which makes the energy of such an object finite. Although it is possible also to construct an example in which the topological charges of the two intersections will be the same, the total topological charge of any finite size defect (for example, formed by several intersecting stripe defects) has to be an integer.[7,9] Therefore at low temperatures the fractional vortices can be present only in the form of bound pairs, whose size is restricted more by the available separations between domain walls in stripe defects rather then by the logarithmic interaction of these objects (which is 64 times weaker than the interaction of ordinary vortices).

With increase of temperature the average separation between the domain walls forming a stripe defect increases, which allows larger separations between the fractional vortices of opposite sign. Above the temperature of vortex-pattern disordering, the restrictions for the distances between fractional vortices related with the separations between domain walls in stripe defects will no longer exist. It looks rather likely[9] that in such a situation one can consider fractional

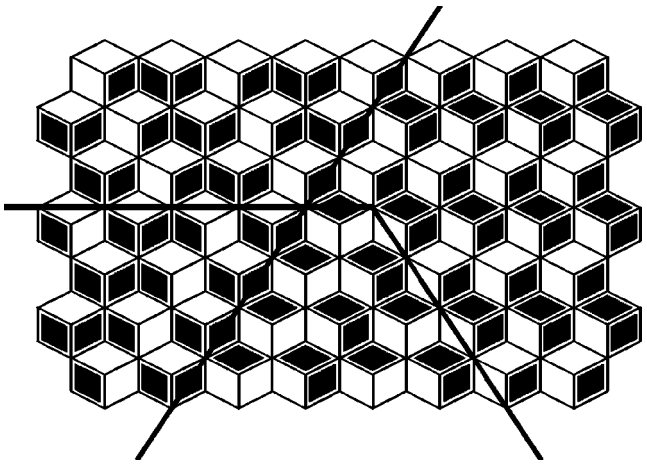

FIG. 7. An example of a fractional vortex.

vortices (at the scales that are large in comparison with the correlation radius) as really logarithmically interacting objects. The same approach may be also applicable to a finite system at $T<T_c$ if its linear size does not exceed the size-dependent correlation radius $r_c(L)$ introduced in Sec. V C. In both cases one can speculate about the possibility of a phase transition related with the unbinding of neutral pairs formed by logarithmically interacting vortex clusters of anomalous sizes.

Substitution of $Q=1/8$ into Eq. (62) allows one to find that the temperature of this phase transition can be estimated as

$$T_{\mathrm{FV}} \approx \frac{\pi}{128}\Gamma_0 = \frac{\pi}{96\sqrt{6}}J \approx 0.013J.$$

This is an estimate from above which neglects the renormalization of Γ by thermal fluctuations. Comparison with the estimate $T_c \gtrsim 0.01J$ obtained in Sec. VI suggests that in the fully frustrated *XY* model on an infinite dice lattice the destruction of phase coherence will be triggered by the disordering of the vortex pattern, which can be expected to occur at a temperature where the logarithmic interaction of fractional vortices at T_c is too weak to keep them bound in pairs.

On the other hand, in a situation when the size of the system is insufficient to exclude the giant finite-size effects leading to the disordering of the vortex pattern at any temperature (see Sec. V C), one can still discuss the possibility of a phase transition (slightly smeared by the finite-size effects), in which the loss of phase coherence will occur as the result of the unbinding of fractional vortices at $T=T_{\mathrm{FV}}\sim 0.01J$. In numerical simulations this phase transition can be observed by analyzing if vortex clusters of anomalous sizes are bound in neutral pairs or not. However, at $T\sim 0.01J$ one should be specially attentive about checking if the time of simulation is sufficient for the equilibration of the vortex subsystem, which at such temperatures will require much longer times than the equilibration of the spin-wave subsystem. It is not clear if in numerical simulations of Ref. 15 (discussed in more detail in Sec. VIII) this condition was really satisfied.

VII. MAGNETIC EFFECTS

It has been already mentioned in the Introduction that the main interest to the uniformly frustrated *XY* models has appeared in relation to their application for the description of Josephson junction arrays in external magnetic field. Since we have found that in the case of the fully frustrated model on a dice lattice the order-from-disorder mechanism for the removal of an accidental degeneracy is extremely inefficient, in a physical situation one should also take into account other possible mechanisms. In the case of a proximity coupled array, the most important of them is related to the magnetic interactions of currents.[25,26,45]

When the proper magnetic fields of currents in the array are taken into account, the Hamiltonian of the frustrated *XY* model should be replaced[46,47] by

$$H = -J\sum_{(jk)} \cos(\theta_{jk} - a_{jk}) + E_{\mathrm{magn}}, \tag{63}$$

where $\theta_{jk}\equiv\varphi_k-\varphi_j-A_{jk}$ includes only the contribution from the external magnetic field, defined by Eq. (2), whereas the analogous contribution from the currents is denoted a_{jk}. The second term in Eq. (63),

$$E_{\mathrm{magn}} = \frac{1}{2}\sum_{\alpha,\beta} L^{-1}_{\alpha\beta}\Phi_\alpha\Phi_\beta, \tag{64}$$

is the energy of the current-induced (screening) magnetic fields expressed in terms of

$$\Phi_\alpha = \frac{\Phi_0}{2\pi}\sum_{\square} a_{jk}, \tag{65}$$

the magnetic fluxes of these fields through the plaquettes of the array (denoted by Greek letters), $L_{\alpha\beta}$ being the matrix of mutual inductances[48] between the plaquettes.

The values of the variables a_{jk} should be found from the minimization of H. The result of the variation of Eq. (63) with respect to a_{jk} can be rewritten as

$$\Phi_\alpha = \sum_\beta L_{\alpha\beta} I_\beta, \tag{66}$$

where I_β is the so-called mesh current[48,49] which can be associated with the plaquette β. The currents in the junctions,

$$I_{jk} = I_0 \sin(\theta_{jk} - a_{jk}),$$

are given by the difference of mesh currents in the two plaquettes, α_{jk} and α'_{jk}, sharing the bond (jk),

$$I_{jk} = I_{\alpha_{jk}} - I_{\alpha'_{jk}}. \tag{67}$$

The substitution of Eq. (66) into Eq. (64) allows one to rewrite it in the more familiar form as

$$E_{\mathrm{magn}} = \frac{1}{2}\sum_{\alpha,\beta} L_{\alpha\beta} I_\alpha I_\beta.$$

In the regime of weak screening one can assume that the values of the currents are not affected by their magnetic fields and calculate E_{magn} replacing I_{jk} by $I^{(0)}_{jk}=I_0\sin\theta_{jk}$. Nonetheless, the calculation of the first term in Eq. (63) with the same accuracy requires one to take into account its dependence of a_{jk}. The contribution to this term which is linear in a_{jk} has a form

$$-\sum_{(jk)} I^{(0)}_{jk} a_{jk},$$

and with the help of Eqs. (64)–(67) can be shown to be equal to $-2E_{\mathrm{magn}}$, where E_{magn} is calculated for the "bare" values of currents, $I^{(0)}_{jk}$. Therefore, in the regime of weak screening, H_{magn}, the total magnetic correction to the Hamiltonian of a Josephson junction array is equal to E_{magn}, but has the opposite sign,

$$H_{\mathrm{magn}} = -E_{\mathrm{magn}}.$$

The comparison of E_{magn} in different periodic states in a fully frustrated superconducting wire network with the dice

lattice geometry has been recently made in Ref. 26. Since in terms of the gauge-invariant phase differences θ_{jk} the structure of these states is in one-to-one correspondence with the ground states of the fully frustrated *XY* model with the same geometry, the same results are also applicable to an array formed by weakly coupled superconducting islands. It follows from the results of Ref. 26 that in arrays the expression for E_{magn} (normalized per a sixfold coordinated site) in the regime of weak screening can be written as

$$E_{\mathrm{magn}} = \frac{\epsilon}{3}\frac{J^2}{E_\Phi}, \tag{68}$$

where

$$E_\Phi = \frac{\Phi_0^2}{4\pi^2 a}$$

is the characteristic energy scale which depends on a, the lattice constant of the array. The numerical coefficient ϵ in Eq. (68) is determined by the structure of the vortex pattern in the considered ground state and can be expressed as a linear combination of the coefficients $\lambda_i > 0$ defining the mutual inductances, $L_i \equiv -\lambda_i a$, between different pairs of plaquettes on a dice lattice. Here $i=1$ corresponds to the nearest neighbors, $i=2$ to the next-to-nearest neighbors, etc.

The main conclusion of Ref. 26 is that in the fully frustrated system with the dice lattice geometry the coefficient ϵ is the largest in the state (c). For example, the numerical coefficient in the expression,

$$\delta H_{\mathrm{magn}} = H^{\mathrm{a}}_{\mathrm{magn}} - H^{\mathrm{c}}_{\mathrm{magn}} = \mu\frac{J^2}{E_\Phi},$$

for the difference between the magnetic energies of the states (a) and (c),

$$\mu = \frac{\epsilon^{\mathrm{c}} - \epsilon^{\mathrm{a}}}{3} = \frac{1}{6}(\lambda_2 + 3\lambda_3 - \lambda_4 - 6\lambda_5 - 5\lambda_7 + 3\lambda_8 + 4\lambda_{10} - \cdots) \approx 0.17,$$

is positive.

For $a = 8\ \mu$m (Ref. 31) $E_\Phi \approx 0.98 \times 10^4$ K, which shows that at $T \sim J$ the differences between the magnetic energies are extremely small, $\delta H_{\mathrm{magn}}/T \lesssim 10^{-4}$, and are even smaller than the differences between the free energies of anharmonic fluctuations. In this estimate we have assumed $T \lesssim 10$ K.

It should be emphasized that in proximity coupled arrays the coupling constant J has a strong temperature dependence in a wide interval of temperatures, so the decrease of the dimensionless temperature $\tau = T/J(T)$ with the decrease of real temperature T is much more strongly influenced by the growth of $J(T)$ than by the decrease of T. Roughly speaking, in the experiments of Ref. 31 the decrease of T by 1 K corresponds to the decrease of τ by one order of magnitude.

This suggests that the importance of magnetic effects rapidly grows with the decrease of τ. Comparison of δH_{magn} with $\delta F_{\mathrm{anh}} = \gamma T^2/J$ shows that the magnetic energy becomes dominant when

$$\tau < \tau_{\mathrm{magn}} = \left(\frac{\mu}{\gamma}\frac{T}{E_\Phi}\right)^{1/3} \approx 0.30,$$

where we have put $T = 5$ K. Thus at $\tau \lesssim 0.1$, where the vortex-pattern ordering can be expected to occur, one can take into account only the magnetic energies of different states (or domain walls), completely neglecting the free energy of anharmonic fluctuations. Therefore the structure of the periodic vortex pattern in the low temperature phase of a proximity coupled array should be of the type (c).

The energy of domain walls separating different versions of state (c) from each other, E_{DW}, will be close to δH_{magn}, which will make the vortex pattern more robust with respect to thermal fluctuations in comparison with the *XY* model. However, any quantitative conclusions about the temperature of the phase transition(s) related to vortex-pattern disordering in this situation are impossible without the detailed analysis of the energies and other properties of the topological excitations in state (c) [analogous to the one performed in Sec. V for state (a)], which goes beyond the limits of this paper. Nonetheless, some increase of the region of stability of the low-temperature phase with the ordered vortex pattern is inevitable, which allows one to conclude that the scenario in which the unbinding of fractional vortices with topological charges $\pm 1/8$ takes place as an independent phase transition is impossible.

Inclusion of the magnetic interactions into analysis improves also the situation with respect to the finite-size effects. For $E_{\mathrm{DW}} \sim J^2/E_\Phi$ the probability to have a domain wall crossing the whole system (of the width L) becomes negligible for

$$L \gg L_c \sim \frac{E_\Phi}{T}\tau^2,$$

which at $\tau \ll 1$ is a much more mild restriction than the one obtained in Sec. V for the *XY* model.

On the other hand, it is known that the magnetic interactions of currents, or, in other words, screening effects, lead to the increase of barriers a vortex has to overcome when moving between the plaquettes of an array.[49] Thus, although the growth of screening effects with a decrease in temperature improves the stability of a vortex-pattern ordering, it simultaneously leads to the further increase of (already exponentially large) times required for the relaxation of the system to equilibrium. This may be one of the reasons why the finite-frequency experiments of Ref. 31 have not demonstrated any signs of a phase transition at $f = 1/2$.

It should also be noted that in the case when the loss of phase coherence is related to dissociation of fractional-vortex pairs, the universal relation[50] for the value of the two-dimensional magnetic penetration depth,[51] Λ, at the transition temperature can be rewritten (in our notation) as

$$\frac{\Lambda(T_{\mathrm{FV}})}{a} = \frac{Q^2}{8}\frac{E_\Phi}{T_{\mathrm{FV}}}.$$

As a consequence, the smearing of the phase transition due to the finiteness of Λ in the case when it is related to unbind-

ing of fractional vortices should be more pronounced then in the case of integer vortices.

VIII. CONCLUSION

In the present work we have investigated the fully frustrated *XY* model on a dice lattice and have demonstrated that the energy of this system is minimized in the highly degenerate family of states (described in Sec. II C), in which the vortices of the same sign are grouped into clusters of three. The accidental degeneracy of these states can be described in terms of the formation of a network of intersecting zero-energy domain walls,[13] whereas the residual entropy related to this degeneracy is proportional to the linear size of the system, as in the case of a honeycomb lattice.[9].

The central result of this paper consists of determining the structure of the periodic vortex pattern which is selected at low temperatures by thermal fluctuations. It is shown in Fig. 3(a). However, this effect is rather weak, being induced only by the anharmonic fluctuations. As a consequence of a hidden gauge symmetry, the free energy of the harmonic fluctuations turns out to be the same for all ground states. The same conclusion is applicable also to quantum generalizations of the model both at a finite and at zero temperature, when one should speak of zero-point fluctuations.

The destruction of the periodic vortex pattern with the increase of temperature is related to the proliferation of domain walls. The dimensionless temperature, $\tau = T/J$, at which the corresponding phase transition can be expected to take place can be estimated as $\tau_c \sim 0.01$, where one factor of 0.1 is related to the smallness of the energy of the particular pointlike defects on domain walls, and the other (which is of the logarithmic origin) to the extreme smallness of the fluctuation-induced free energy of zero-energy domains walls. The analysis of possible scenarios suggests that the loss of phase coherence in the considered system can be expected to take place at the same temperature as the disordering of the vortex pattern.

The extreme smallness of the fluctuation-induced free energy of domain walls will manifest itself also in the huge prominence of the finite-size effects consisting of the appearance of domain walls crossing the whole system and leading to the disordering of the vortex pattern even at $\tau < \tau_c$. As a consequence, even at the "optimal" temperature, $\tau \approx 0.8\tau_c$, the linear size of the system required to observe the vortex-pattern ordering should be much larger than $r_c^{\min} \approx 2 \times 10^4$. However, in smaller systems one can still discuss a possibility for the observation of a phase transition related to the loss of phase coherence and consisting of unbinding of pairs of logarithmically interacting vortex clusters of anomalous sizes, which can be expected to happen at $\tau_{\mathrm{FV}} \sim 0.01$.

Our conclusions are consistent with the results of the numerical simulations of the same model by Cataudella and Fazio[15] who have investigated the temperatures down to $\tau = 0.01$ and have found no signs of vortex-pattern ordering. The results presented in Sec. V demonstrate that even if the lowest temperatures investigated in Ref. 15 were indeed below τ_c, the size of the system was definitely not sufficient for the observation of such an ordering. In the notation based on counting only the sixfold coordinated sites (used in this work), the largest size of the system analyzed in Ref. 15 corresponds to 56×42, whereas the majority of the data has been taken at 24×18. It seems rather likely that analogous simulations of a $10^5 \times 10^5$ system, which may be required for the observation of vortex-pattern ordering in the fully frustrated *XY* model on a dice lattice, can become possible only with the further development of computational abilities.

Another result of the numerical simulations of Ref. 15 is related to the dynamical properties of the system (which were not discussed in this paper) and consists of finding below $\tau_* \approx 0.06$ the signs of a glassy behavior. Namely, the relaxation of the total energy at $\tau < \tau_*$ becomes logarithmic in time (in contrast to the exponential relaxation at $\tau > \tau_*$), whereas the behavior of the autocorrelation function of the variables θ_{jk} demonstrates a dependence on the waiting time.

One can certainly make an attempt to relate this observation to the specific features of the considered system. For the temperatures and system sizes analyzed in Ref. 15 one can safely neglect the fluctuation-induced free energy of zero-energy domain walls and treat them as objects with zero free energy. It seems rather likely then that the typical state obtained after cooling down the system from $\tau \sim 1$ to $\tau \ll E_K/J$ can be described as a network formed by zero-energy domain walls, which contains a large number of pointlike defects, such as kinks and intersections, which cost an additional energy. We know that the intersections with zero energy are also possible [see Fig. 3(f)], but one can expect that the majority of the intersections formed during cooling down from a disordered state will not have the optimal structure necessary for that.

The glassy behavior can be then expected from the necessity of the disentanglement of this domain wall network with the decrease of temperature. For different temperatures above τ_c, the equilibrium concentration of pointlike defects should be different. However, in contrast to kinks on a domain wall whose number can be changed due to annihilation of two kinks of opposite signs (which may be a relatively fast process), to change the number of the intersections of domain walls one has to change the number of these walls, which will require much longer times than the annihilation of kinks. In particular, it seems rather likely that the processes related to the annihilation of zero-energy domain walls crossing the whole system will be characterized by relaxation times diverging with the system size, providing thus a source for a genuine glasslike behavior.

On the other hand, even if the times characterizing the relaxation of the vortex pattern are not divergent in the thermodynamic limit and are restricted only by the barriers whose typical height remains of the order of *J*, this already can be the source for a glassylike behavior (associated with a wide distribution of such barriers) at $\tau \ll 1$ in a wide interval of times. For example, $\exp(1/0.05) \sim 10^9$, whereas in Ref. 15 the anomalous relaxation has been studied only at much shorter times. In such a case one can argue that the observation of a glassylike behavior in the considered *XY* model is possible due to a combination of three factors, namely, (i) the existence of zero-energy domain walls, (ii) the special ineffectiveness of the order-from-disorder mechanism for the

removal of an accidental degeneracy, and (iii) the anomalously low transition temperature ($\tau_c \sim 0.01$). However, the choice between the two scenarios (genuine glass vs the dynamical freezing of vortex relaxation) should be made on the basis of a much more detailed analysis of the domain-walls disentanglement.

In the experimental situation, the magnetic interactions of currents in a Josephson junction array will be of greater importance for the stabilization of a particular vortex pattern then the anharmonic fluctuations. This mechanism leads to the selection of the pattern shown in Fig. 3(c) and makes the periodic vortex pattern less vulnerable with respect to fluctuations.

ACKNOWLEDGMENTS

The author is grateful to B. Douçot and P. Martinoli for numerous useful discussions. This work has been supported in part by the Program "Quantum Macrophysics" of the Russian Academy of Sciences, by the Program "Scientific Schools of the Russian Federation" (Grant No. 1715.2003.2), and by the Swiss National Science Foundation.

[1] S. Teitel and C. Jayaprakash, Phys. Rev. Lett. **51**, 1999 (1983).
[2] For a review, see, for example, P. Martinoli and Ch. Leemann, J. Low Temp. Phys. **118**, 699 (2000); or R. S. Newrock, C. J. Lobb, U. Geigenmüller, and M. Octavio, in *Solid State Physics*, Vol. 54, edited by H. Ehrenreich and F. Spaepen (Academic Press, San Diego, 2000), p. 263.
[3] S. Teitel and C. Jayaprakash, Phys. Rev. B **27**, 598 (1983).
[4] D. H. Lee, R. G. Caflisch, J. D. Joannopoulos, and F. Y. Wu, Phys. Rev. B **29**, 2680 (1984).
[5] S. Miyashita and J. Shiba, J. Phys. Soc. Jpn. **53**, 1145 (1984).
[6] W. Y. Shih and D. Stroud, Phys. Rev. B **32**, 158 (1985); S. Teitel and C. Jayaprakash, J. Phys. (France) Lett. **46**, L33 (1985).
[7] T. C. Halsey, J. Phys. C **18**, 2437 (1985).
[8] S. E. Korshunov and G. V. Uimin, J. Stat. Phys. **43**, 1 (1986).
[9] S. E. Korshunov, J. Stat. Phys. **43**, 17 (1986).
[10] J.-R. Lee and S. Teitel, Phys. Rev. Lett. **66**, 2100 (1991); Phys. Rev. B **46**, 3247 (1992).
[11] S. Lee and K.-C. Lee, Phys. Rev. B **49**, 15 184 (1994); **57**, 8472 (1998); P. Olsson, Phys. Rev. Lett. **75**, 2758 (1995); **77**, 4850 (1996); Phys. Rev. B **55**, 3585 (1997); V. Cataudella and M. Nicodemi, Physica A **233**, 293 (1996); Y. Ozeki and N. Ito, Phys. Rev. B **68**, 054414 (2003).
[12] V. Cataudella, G. Franzese, S. E. Korshunov, and R. Fazio, Physica B **284-288**, 431 (2000); G. Franzese, V. Cataudella, S. E. Korshunov, and R. Fazio, Phys. Rev. B **62**, R9287 (2000).
[13] S. E. Korshunov, Phys. Rev. B **63**, 134503 (2001).
[14] S. E. Korshunov, Phys. Rev. Lett. **88**, 167007 (2002).
[15] V. Cataudella and R. Fazio, Europhys. Lett. **61**, 341 (2003).
[16] S. E. Korshunov and B. Douçot, Phys. Rev. Lett. **93**, 097003 (2004).
[17] J. Villain, J. Phys. C **10**, 1717 (1977).
[18] These domain walls can be compared to stacking faults in close-packed structures formed by identical three-dimensional spheres.
[19] J. Villain, R. Bidaux, J. P. Carton, and R. Conte, J. Phys. (France) **41**, 1263 (1980).
[20] E. F. Shender, Zh. Eksp. Teor. Fiz. **83**, 326 (1982) [Sov. Phys. JETP **56**, 178 (1982)].
[21] H. Kawamura, J. Phys. Soc. Jpn. **53**, 2452 (1984); S. E. Korshunov, Pis'ma Zh. Eksp. Teor. Fiz. **41**, 525 (1985) [JETP Lett. **41**, 641 (1985)]; J. Phys. C **19**, 5927 (1986); C. L. Henley, J. Appl. Phys. **61**, 3962 (1987); Phys. Rev. Lett. **62**, 2056 (1989).
[22] S. E. Korshunov, A. Vallat, and H. Beck, Phys. Rev. B **51**, 3071 (1995).
[23] T. Horiguchi and C. C. Chen, J. Math. Phys. **15**, 659 (1974); B. Sutherland, Phys. Rev. B **34**, 5208 (1986).
[24] R. Meyer, S. E. Korshunov, Ch. Leemann, and P. Martinoli, Phys. Rev. B **66**, 104503 (2002).
[25] K. Park and D. A. Huse, Phys. Rev. B **64**, 134522 (2001).
[26] S. E. Korshunov and B. Douçot, Phys. Rev. B **70**, 134507 (2004).
[27] J. Vidal, R. Mosseri, and B. Douçot, Phys. Rev. Lett. **81**, 5888 (1998).
[28] P. G. de Gennes, C. R. Seances Acad. Sci., Ser. 2 **292**, 9 (1981); **292**, 291 (1981); S. Alexander, Phys. Rev. B **27**, 1541 (1983).
[29] C. C. Abilio, P. Butaud, Th. Fournier, B. Pannetier, J. Vidal, S. Tedesco, and B. Dalzotto, Phys. Rev. Lett. **83**, 5102 (1999).
[30] B. Pannetier, C. C. Abilio, E. Serret, T. Fournier, P. Butaud, and J. Vidal, Physica C **352**, 41 (2001); E. Serret, P. Butaud, and B. Pannetier, Europhys. Lett. **59**, 225 (2002); E. Serret, Ph.D. thesis, Grenoble, 2002.
[31] M. Tesei, R. Théron, and P. Martinoli (unpublished).
[32] Although in Sec. III quantum generalizations of the same model are also considered, the term "Hamiltonian" in this paper is always used as in statistical mechanics, to denote the expression for the static energy of the system, and not as in quantum mechanics.
[33] M. Wolf and K. D. Schotte, J. Phys. A **21**, 2195 (1988).
[34] In all examples shown in Fig. 3 all domain walls of the type I (if present) are horizontal.
[35] L. Onsager, Phys. Rev. **65**, 117 (1944).
[36] S. E. Korshunov, Phys. Rev. B **65**, 054416 (2002).
[37] The disordering of the vortex pattern can also be a multistage process, like, for example, in the $f \ll 1$ limit, when the behavior of the system can be described in terms of vortex crystal depinning and melting (Ref. 38).
[38] M. Franz and S. Teitel, Phys. Rev. Lett. **73**, 480 (1994); Phys. Rev. B **51**, 6551 (1995); S. Hattel and J. Wheatley, *ibid.* **50**, 16 590 (1994); **51**, 11 951 (1995); J. P. Straley, A. Y. Morozov, and E. B. Kolomeisky, Phys. Rev. Lett. **79**, 2534 (1997).
[39] V. L. Berezinskii, Zh. Eksp. Teor. Fiz. **61**, 1144 (1971) [Sov. Phys. JETP **34**, 610 (1972)]; J. M. Kosterlitz and D. J. Thouless, J. Phys. C **5**, L124 (1972); **6**, 1181 (1973); J. M. Kosterlitz, *ibid.* **7**, 1046 (1974).
[40] D. R. Nelson and J. M. Kosterlitz, Phys. Rev. Lett. **39**, 1201 (1977).
[41] S. E. Korshunov, Phys. Rev. Lett. **94**, 087001 (2005).
[42] M. K. Ko, S. J. Lee, J. Lee, and B. Kim, Phys. Rev. E **67**, 046120 (2003).

[43] Y. H. Li and S. Teitel, Phys. Rev. Lett. **65**, 2595 (1990); C. Denniston and C. Tang, *ibid.* **79**, 451 (1997); Phys. Rev. B **58**, 6591 (1998).

[44] S. Y. Park, M. Y. Choi, B. J. Kim, G. S. Jeon, and J. S. Chung, Phys. Rev. Lett. **85**, 3484 (2000).

[45] In the case of a SIS (superconductor-insulator-superconductor) array, it is also necessary to consider another mechanism of the removal of the accidental degeneracy related to the anharmonic quantum fluctuations.

[46] D. Stroud and S. Kivelson, Phys. Rev. B **35**, 3478 (1987).

[47] D. Domínguez and J. V. José, Phys. Rev. Lett. **69**, 514 (1992).

[48] C. A. Desoer and E. S. Kuh, *Basic Circuit Theory* (McGraw-Hill, New York, 1969).

[49] J. R. Phillips, H. S. J. van der Zant, J. White, and T. P. Orlando, Phys. Rev. B **47**, 5219 (1993).

[50] M. R. Beasley, J. E. Mooij, and T. P. Orlando, Phys. Rev. Lett. **42**, 1165 (1979).

[51] This is the length at which the logarithmical interaction of vortices is screened (Refs. 46 and 52).

[52] J. Pearl, in *Low Temperature Physics—LT9*, edited by J. D. Daunt, D. O. Edwards, F. J. Milford, and M. Yacub (Plenum Press, New York, 1965), p. 566.